

LASER INTERFEROMETER GRAVITATIONAL WAVE OBSERVATORY
-LIGO-
CALIFORNIA INSTITUTE OF TECHNOLOGY
MASSACHUSETTS INSTITUTE OF TECHNOLOGY

Technical Note
12/13/2004

LIGO-T040231-00-R

**Development of Optical lever system of
the 40 meter interferometer**

Fumiko Kawazoe

This is an internal working note
of the LIGO Project.

California Institute of Technology
LIGO Project – MS 51-33
Pasadena CA 91125
Phone (626) 395-2129
Fax (626) 304-9834
E-mail: info@ligo.caltech.edu

Massachusetts Institute of Technology
LIGO Project – MS 20B-145
Cambridge, MA 01239
Phone (617) 253-4824
Fax (617) 253-7014
E-mail: info@ligo.mit.edu

WWW: <http://www.ligo.caltech.edu>

ABSTRACT

LIGO's 40 meter interferometer is now testing a Resonant Sideband Extraction scheme for Advanced LIGO. In order for the interferometer to work properly one of the most important things is to maintain the position and orientation of the suspended optics. The Optical Sensor and Electro Magnetic actuator damping system controls the position of the optics and the Optical lever system is used to monitor the angular orientation of the optics. This document reports on work done on commissioning the system, calibrating its response, characterizing noise in the system, and closing the control loop during the summer of 2003 to the summer of 2004.

KEYWORDS

Optical lever
Suspended optics
40 meter interferometer

ACKNOWLEDGEMENTS

I would like to thank Professor Alan J. Weinstein for giving me the wonderful opportunity to work in the 40 meter lab and his great advice. I would also like to thank my adviser at NAOJ Seiji Kawamura for giving me the great chance to participate in the 40 meter project with him. And many thanks to Osamu Miyakawa for giving me useful advice on my project and Rana Adhikari for explaining how the Oplev filters at the Hanford site work, it was very helpful. Lots of thanks to Mike Smith, Steve Vass, Bob Taylor, Ben Abbott and Jay Heefner for their helps.

CONTENTS

1	Introduction	4
1.1	Gravitational waves.....	4
1.2	Principle of detection.....	5
1.3	World project.....	5
1.4	LIGO's 40 Meter interferometer.....	6
1.5	Mirror control.....	6
2	Optical lever system	7
2.1	Commissioning the Optical lever system.....	8
2.2	Calibrating the Optical lever response.....	9
2.2.1	The measurement principle.....	10
2.2.2	Calibration method.....	13
2.2.3	The result.....	17
3	Optical lever system sensitivity	23
3.1	Expected noise sources in the system.....	23
3.2	Noise characterization.....	24
4	Controlling the optics	27
4.1	Q-factor.....	27
4.2	Designing digital filters for Optical lever control loop.....	31
4.3	In-loop noise measurement.....	32
4.4	The result.....	32
5	Future work.....	46
6	Conclusion.....	47

1 Introduction

1.1 Gravitational waves

Gravitational waves are ripples in space-time produced by accelerating masses such as celestial objects. Einstein predicted the existence of gravitational waves in 1916 in his General theory of relativity. As a consequence of Einstein's equation under the approximation that space-time is nearly flat a disturbance of the curvature of space-time propagates at the speed of light. The perturbation of flat space-time is represented by $h_{\mu\nu}$. As a wave passes it changes the space-time interval, stretching it in one direction (x-axis) and compressing it in the other (y-axis). Figure 1 visualizes the effect of a gravitational wave on a set of free-falling test masses. The wave described in Fig. 1 propagates vertically through the paper (z-axis) and the polarization states are orthogonal to the direction of the propagation (x-y plane). These states are called plus and cross and their polarization axes are $\pi/4$ rotated with respect to each other as shown in Fig. 1.

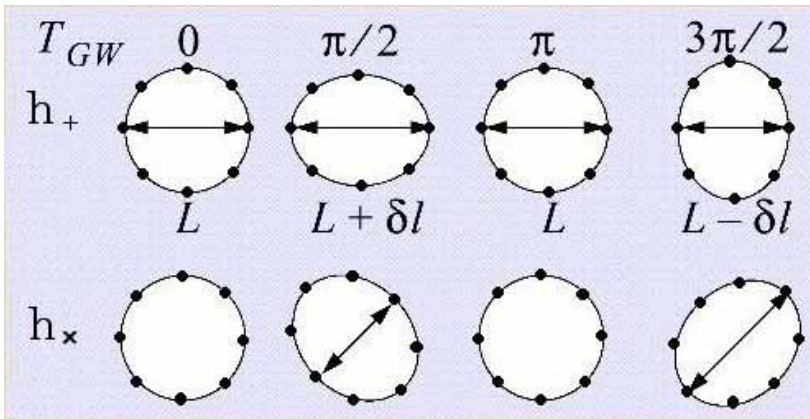


Fig. 1: Two polarization states of a gravitational wave passing through the plane of the paper. It shows how the wave stretches and compresses the distance between test masses.

The ratio of the distance between test masses to the deviation caused by a wave is expressed as a strain h . The strain is very small, making the direct detection of gravitational waves very challenging. For example waves emitted by a binary neutron star pair each of whose mass is 1.4 solar masses, located about 15 Mega pc away would emit a gravitational wave whose strain is $h \approx 1 \times 10^{-21}$.

1.2 Principle of detection

To directly detect the strain caused by gravitational waves, a Michelson interferometer is a useful device since it can measure the difference in length of the two arms. As shown in Fig. 2 when a wave passes through the Michelson interferometer it stretches one arm and shrinks the other. The interferometer is set in such a way that when it is free from gravitational waves the output port is kept dark (dark port). The length change caused by a gravitational wave will cause a phase shift of the light and will appear as the change in power at the dark port, producing the signal. Because the strain is a ratio between the displacement a wave causes (ΔL) and the interferometer arm length (L) with a larger L , the detector's sensitivity to the signal can be increased.

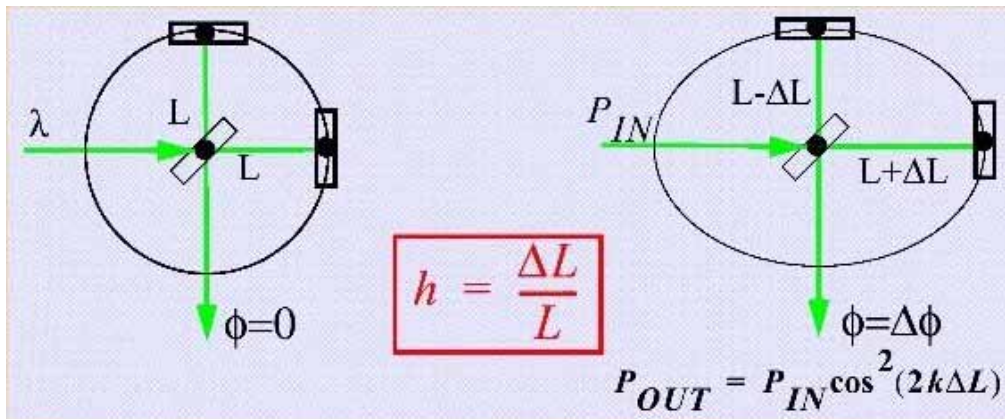


Fig. 2: Michelson interferometer as a gravitational wave detector

1.3 World project

There are several large interferometers in the world such as LIGO, VIRGO, GEO and TAMA. These are the first generation detectors some of which are currently operating. The second generation detectors are also planned to be operated in the near future and among them are Advanced LIGO and LCGT.

1.4 LIGO's 40 Meter Interferometer

LIGO's 40 Meter interferometer is now testing a full Resonant Sideband Extraction (RSE) before the technique is employed in Advanced LIGO. The 40 meter interferometer has the same optical settings except for the arm length which is shorter than in Advanced LIGO by a factor of 100.

1.5 Mirror control

40 meter interferometer uses suspended optics as shown in Fig. 3-a and 3-b so that they will behave as free-falling test masses well above the resonant frequency of the pendulum. As shown in Fig. 3-a and 3-b the suspended optic behaves as a pendulum in pitch, yaw, and position. In theory the suspended optics act as free-falling mass but in reality they are shaken constantly by noise sources. Thus it is necessary to monitor and control the optic system for the interferometer to be operated properly.

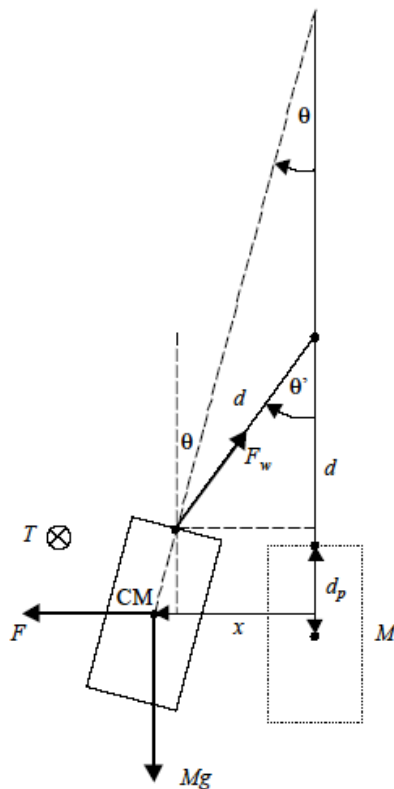


Fig. 3-a: Suspended optic acting as a pendulum in position and pitch

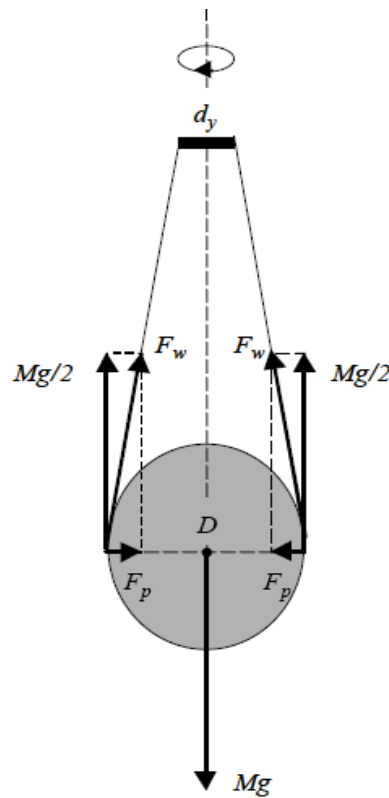


Fig. 3-b: Suspended optic acting as a pendulum in yaw

In the 40 meter interferometer there is a main mirror control system referred to as Digital Suspension Controller which consists of Optical Sensor and Electro Magnetic actuator (OSEM) sensors, OSEM coils, and Optical lever (Oplev) systems. OSEM sensors monitor the suspended optic's position, pitch, and yaw motion by the position sensor which is composed of a set of LED's and photodetectors, and controls them by the set of coils and magnets. Because the system is on the same optical table as the suspended optic they share the same reference. On the other hand the Oplev system is placed outside the optical table where the optics are on, thus it has a different reference. The oplev system is used to monitor the angular orientation of the optics and to set a reference whenever there is a significant change in optics settings.

2 Optical lever system

An optical lever is a useful device to detect a small displacement in an angular position by magnifying and converting the angular displacement into a position change on a position sensitive photodetector. (See Fig. 4).

At present each of the seven optics used in the 40 meter interferometer has an oplev system to monitor their angle motion and maintain the angle orientation.

An oplev system is composed of an optical part and an electronics part. The optical part has a 670nm laser diode, steering mirrors to guide the beam, and a Quadrant Photo Detector (QPD) which is designed to be sensitive to position displacement. It detects a small motion in pitch or yaw by sending a beam to a suspended mirror and reading its signal on a QPD as shown in Fig 4. When there is a small angle displacement of θ either in pitch or yaw motion the position displacement on the QPD will be $\Delta x = 2R\theta$. In a real system there are steering mirrors in the beam path to guide the beam. The electronics part is composed of Oplev interface board, Pentax 16-bit ADC, Pentium CPU, Linux computer, EPICS display, and wires that connect them.

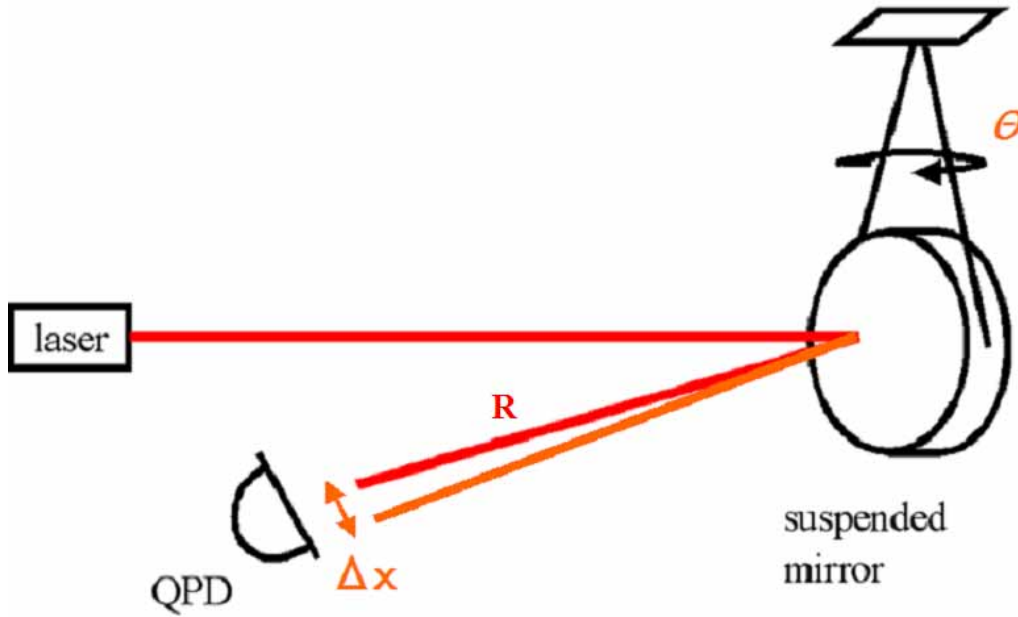


Fig. 4: Detection of a small angular motion using the Optical Lever

Using this system as not only a monitoring device but also an auxiliary servo control system for angle orientation has been considered.

My work includes resetting up the existing Oplev systems, calibrating their angle motion to QPD response, characterizing noise in the system, designing servo filters, and implementing them into the system to help control the optics.

2.1 Commissioning the Optical lever system

All five optics (ITMX, ETMX, ITMY, ETMY, and BS) had Oplev systems installed previously but the beam intensities were too weak to be detected on some QPDs and the beam paths needed to be changed so that the QPDs would have enough power on them.

The change made to the path is described in Chart 1. With the new changes the intensities of the beam on the QPDs were increased by an order of magnitude and all of the five Oplev systems have enough power to be detected on the QPDs.

Optics	Change made to the system	Incident beam path length (cm)	Returning beam path length (cm)	Total beam path length (cm)
ITMX	<ul style="list-style-type: none"> No significant change 	203.6	270.2	473.8
ETMX	<ul style="list-style-type: none"> Beam used to hit HR side of the optic → it hits the AR side of it Number of steering mirror in the path reduced from 5 to 3 	133.6	167.5	301.1
ITMY	<ul style="list-style-type: none"> No significant change 	251.5	181.9	433.4
ETMY	<ul style="list-style-type: none"> Beam used to hit the HR side of the optic → it hits the AR side of it Number of steering mirror in the path reduced from 5 to 3 	157.4	192.8	350.2
BS	<ul style="list-style-type: none"> Number of steering mirror in the path reduced from 8 to 7 	251.1	363.9	615

Chart 1: Changes made to the existing Oplev system

2.2 Calibrating the Optical lever response

The EPICS display shows the QPD readout as shown in Fig. 5. The QPD has 4 segments as shown in part A. The pitch and yaw values are calculated by comparing the amount of power on each of the segments as shown in part B and normalized with the total power on the QPD. The values go into the control loop as an input as shown in part C then the offset will be added to it as shown in part D. The pitch and yaw signals are calculated and shown in part E.

The values show how much the beam is off from the center of the QPD and not directly the angular orientation of the optic. Thus it is necessary to know how much optic angular motion gives how much displacement on the QPD by calibrating the QPD response to the optics angular orientation.

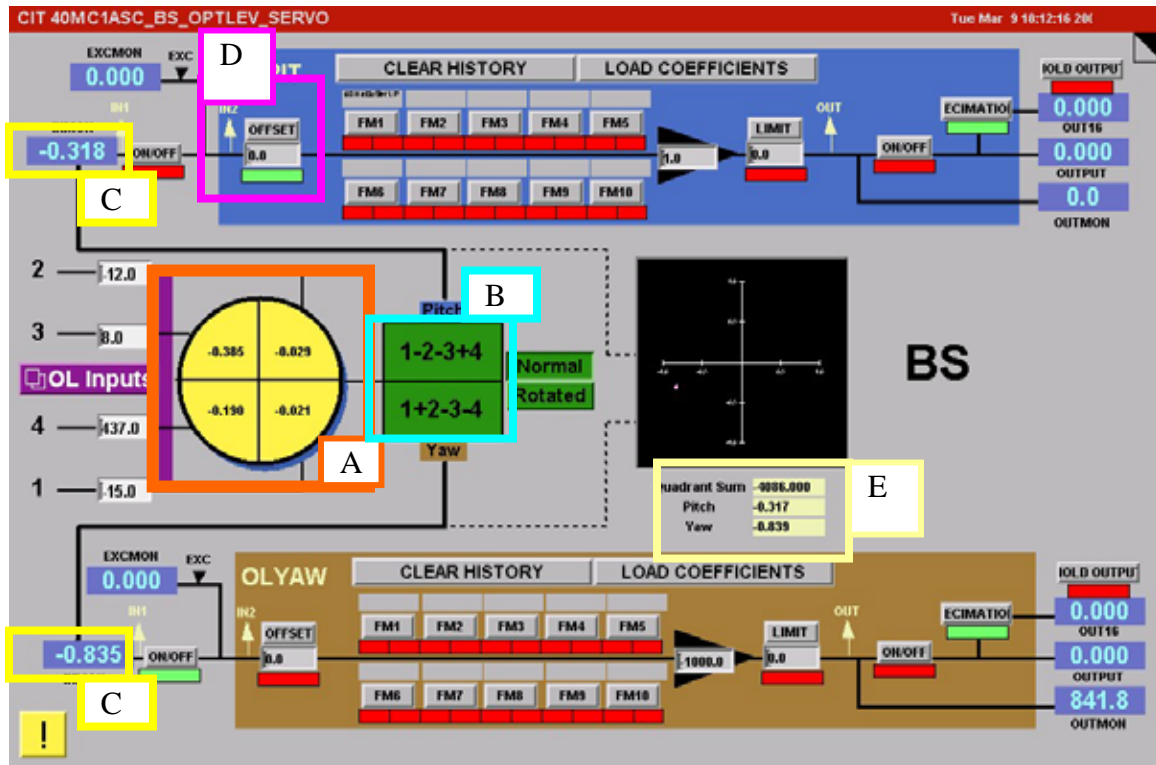


Fig. 5 : The EPICS screen reading out the signal

2.2.1 The measurement principle

In order to calibrate the response of the QPD to the angular motion of the optic, the signals are read from the EPICS display when a known small position displacement is added to the beam path. Then the angular displacement of the optics that would give the same position displacement to the beam will be calculated.

To give a known small position displacement, a glass plate is a useful device because it gives a small shift to the exit beam due to the light refraction effect. Snell's law describes how much shift the glass plate adds to the incident beam and when the wave length of the beam, the incident angle, and the index of refraction of the air and

the glass plate are known, the angular displacement can be calculated. Figure 6 shows how the beam is shifted after passing through the glass plate.

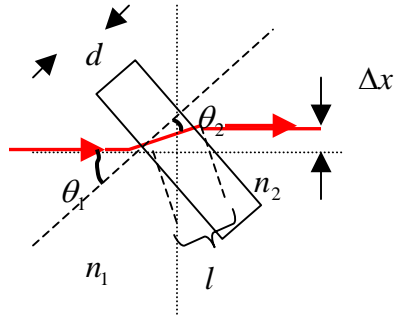


Fig. 6: Beam shift caused by the glass plate

According to Snell's law, the relationship between angles of incidence and refraction for the beam can be written as

$$\frac{n_1}{n_2} = \frac{\sin \theta_2}{\sin \theta_1}$$

From which the displacement Δx added to the incident beam can be calculated as follows:

$$\frac{n_1}{n_2} = \frac{\sin \theta_2}{\sin \theta_1}$$

where

θ_1 ... angle of incidence

n_1 ... index of refraction of air = 1.0003

θ_2 ... angle of refraction

n_2 ... index of refraction of the glass plate (BK7)

for 670nm wave length = 1.51391

d ... thickness of the glass plate = 6.35mm

$$\rightarrow \sin \theta_2 = \frac{n_1}{n_2} \times \sin \theta_1$$

$$l \cos \theta_2 = d$$

$$\rightarrow l = \frac{d}{\cos \theta_2}$$

$$= \frac{d}{\sqrt{1 - \left(\frac{n_1}{n_2} \sin \theta_1\right)^2}}$$

$$\Delta x = l \sin(\theta_1 - \theta_2)$$

$$= d \sin \theta_1 \left(1 - \frac{n_1}{n_2} \frac{\cos \theta_1}{\sqrt{1 - \left(\frac{n_1}{n_2} \sin \theta_1\right)^2}}\right) \quad \left(0 \leq \theta \leq \frac{\pi}{2}\right)$$

From the position displacement on the photo detector Δx , the angular displacement of the optic that would give the same displacement can be calculated. Figure 7 shows how the angular displacement causes the position displacement.



Fig. 7: Position displacement of the beam on a QPD caused by the angular displacement of the optic

From Fig.7 the angular displacement $\Delta\theta$ is calculated as follows:

$$R \times 2\Delta\theta = \Delta x$$

where

$$\rightarrow \Delta\theta = \frac{\Delta x}{2R}$$

φangle of incidence

Δx ... position displacement

$$= c \times V$$

Rreturn beam path length

θangular displacement of the optic

ccalibration factor given in the table in section 2.2.3

Vpitch or yaw reading from the EPICS screen,

Figure 5, part C.

2.2.2 Calibration method

The measurement for all 7 optics was done in the way described below.

Yaw measurement

1: The offset of the oplev quadrant input was adjusted so that when there is no light on the QPD the output monitor (c1:sus-suspension name_OL1~4_OUTMON) oscillates around 0. (See Fig. 8). The output monitor port (c1:sus-suspension name_OL1~4_OUTMON) shows values about 6500 times larger than the actual output (c1:sus-suspension name_OL1~4_OUTPUT) so that it is more useful to read this value when there is little light on the QPDs as shown in Fig. 9.

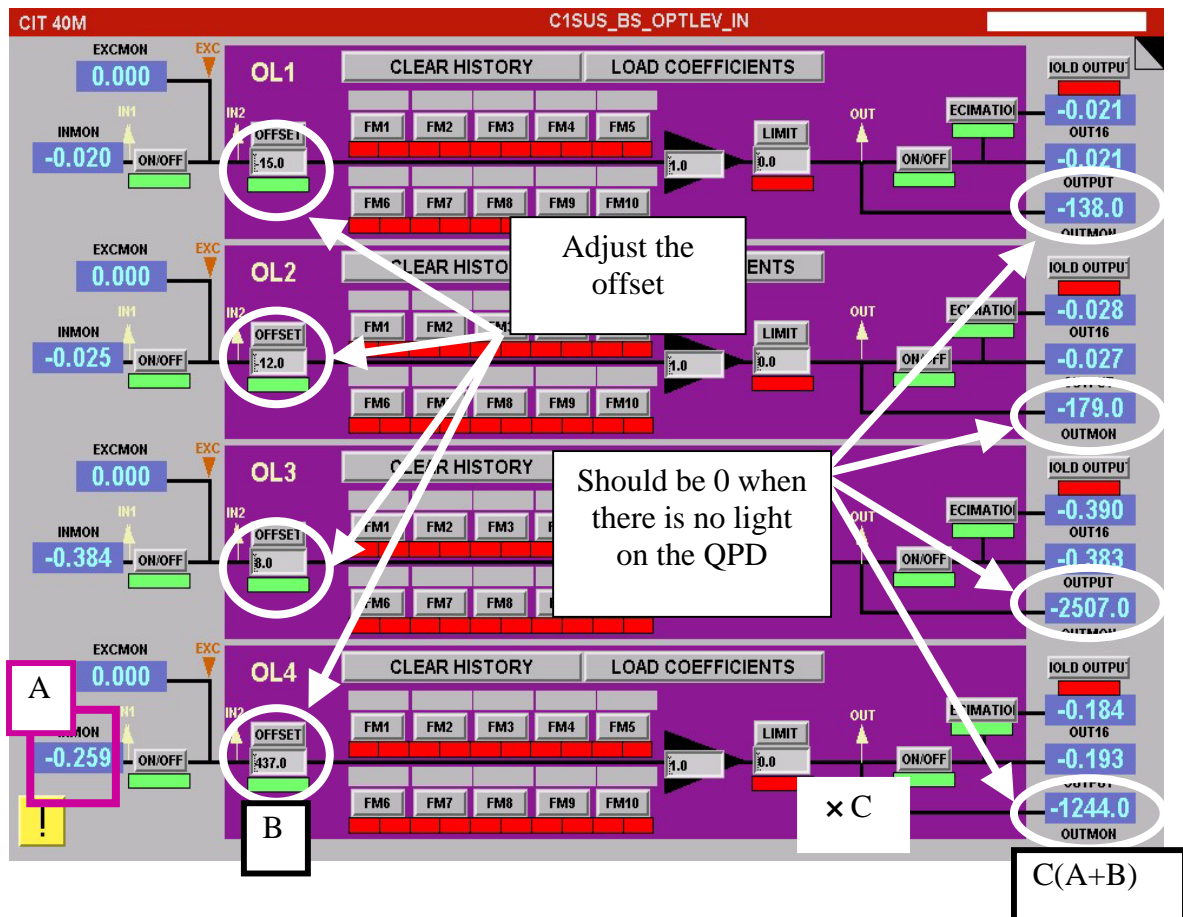


Fig. 8 : The EPICS screen which displays the offset (B) and the input (A)

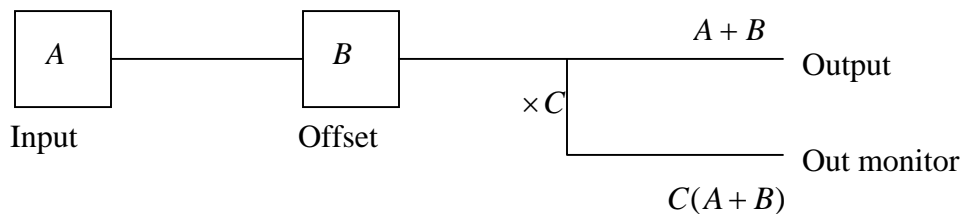


Fig. 9: Schematic diagram which shows the signal flow from the input to the output. Here C is about 6500 and it is useful to use the out monitor port when there is little light on the QPD.

2: The beam was centered on the QPD by getting the oplev pitch and yaw readings close to 0.

3: The glass plate on a rotary mount was placed in front of the QPD as shown in Fig. 10. The distance between them is approximately 10cm. Since the glass plate is slightly wedged it was made sure the wedge is in vertical direction so that the initial beam is horizontally parallel to the outgoing beam as shown in Appendix A.

4: Placing the glass plate in front of the QPD may change the beam height a little. First the beam on the glass plate was centered and it was made sure that the beam was horizontally centered on the QPD. Then the beam height was readjusted so that it hits the center of the QPD via the oplev readback.

5: The yaw value was read from the output port (C1:SUS-suspension name_OL_yaw) as the part B of the glass plate in Fig. 10 was rotated every 2 degrees in both positive and negative angle until the signal gets saturated.

6: Plot the data

The data were plotted and only that of the linear region were selected to fit to a linear function ($f(x) = a \times x$). By fitting the data to the function the calibration factor was obtained.

Pitch measurement

1: The same thing was done except in doing step 3 it was made sure that the wedge is in the horizontal direction so that the incident beam is vertically parallel to the exit beam.

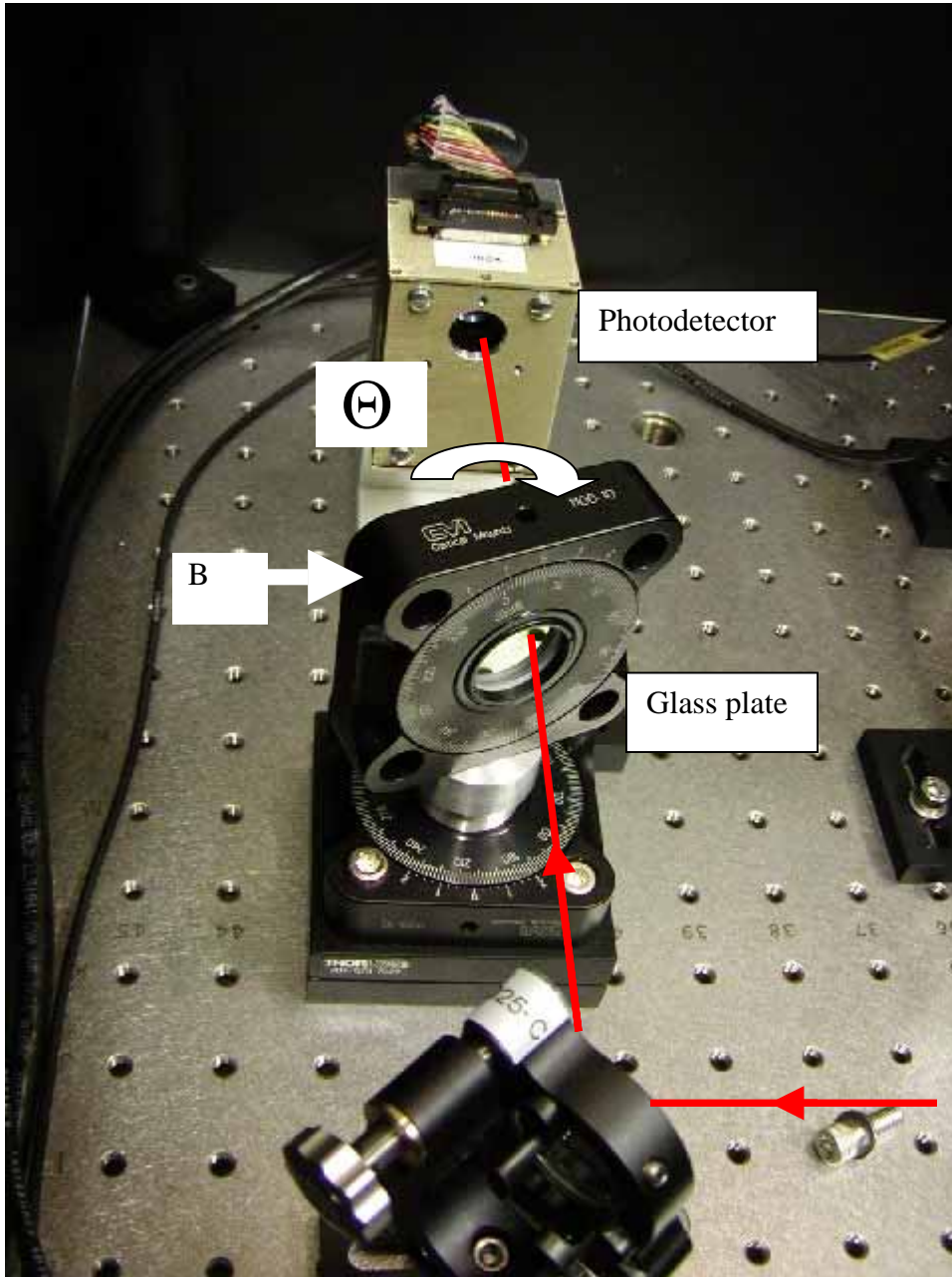


Fig. 10 : Setup of the Yaw measurement

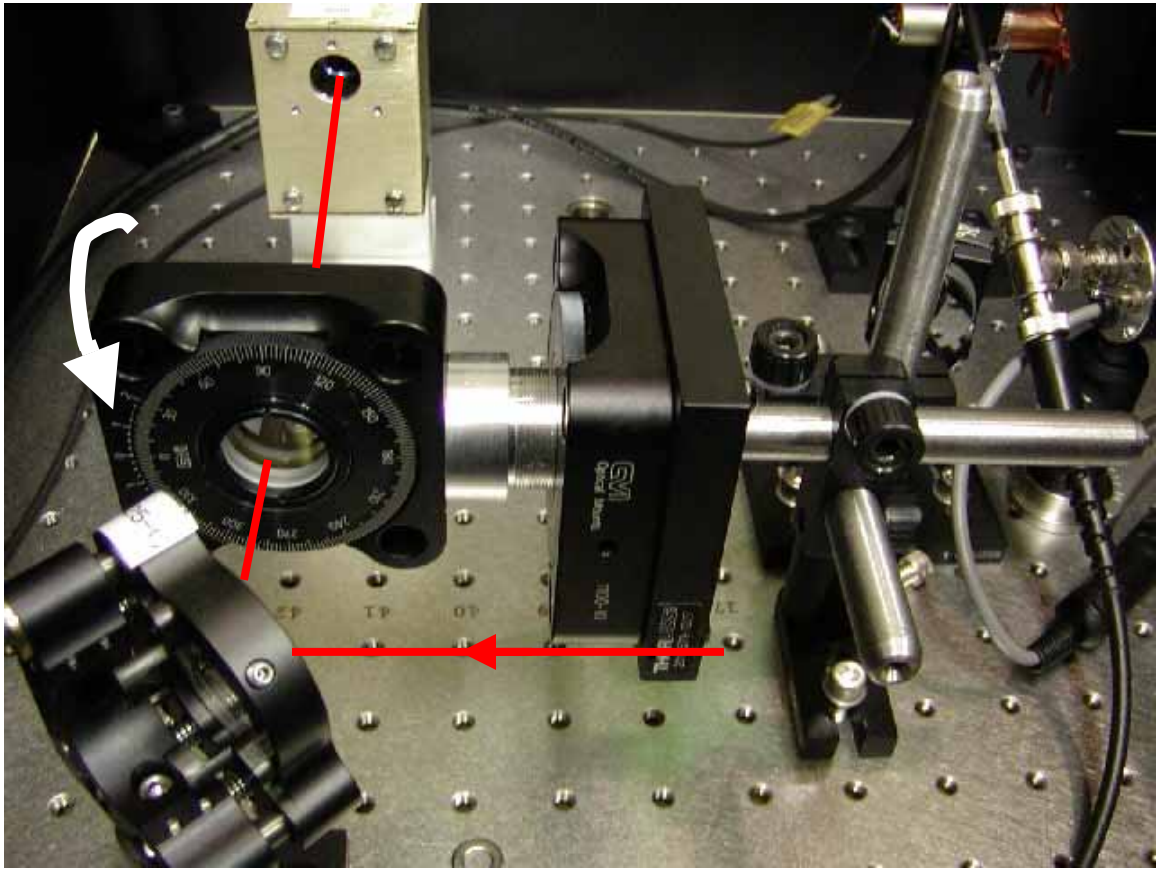


Fig. 11 : Setup of the Pitch measurement

2.2.3 The result

The plots of the Oplev response as recorded on the EPICS screen (Fig. 5, part C) to angular displacement are shown in Fig.12 through Fig.16.

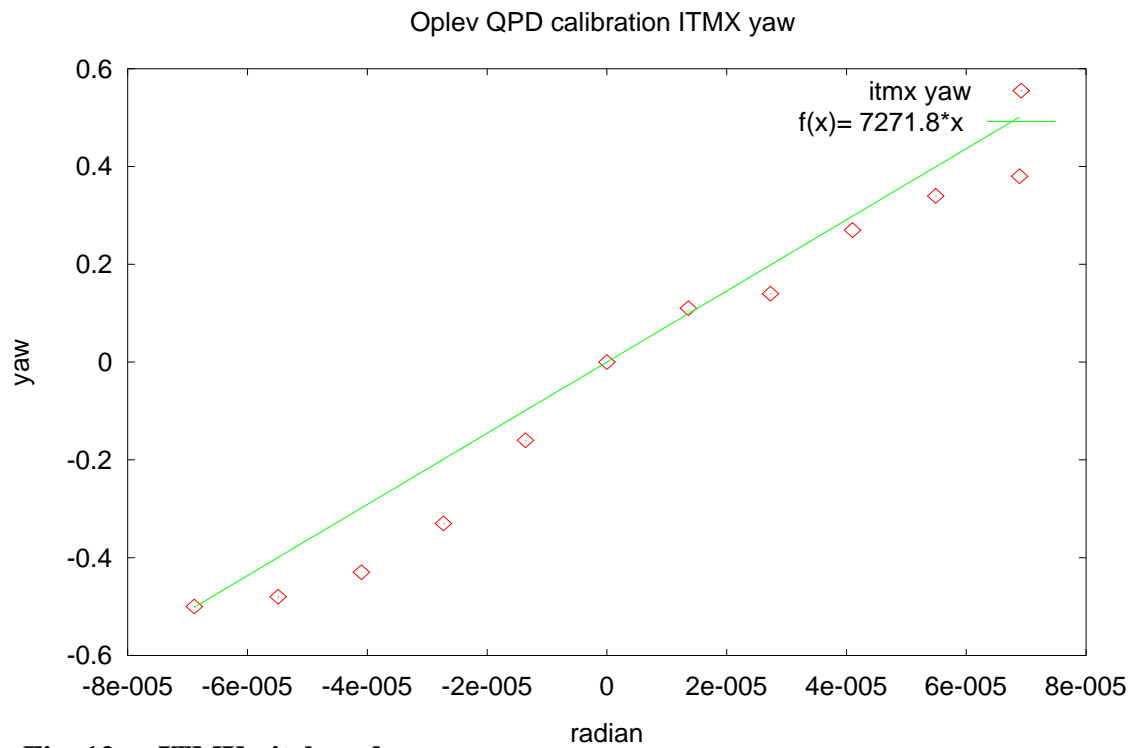
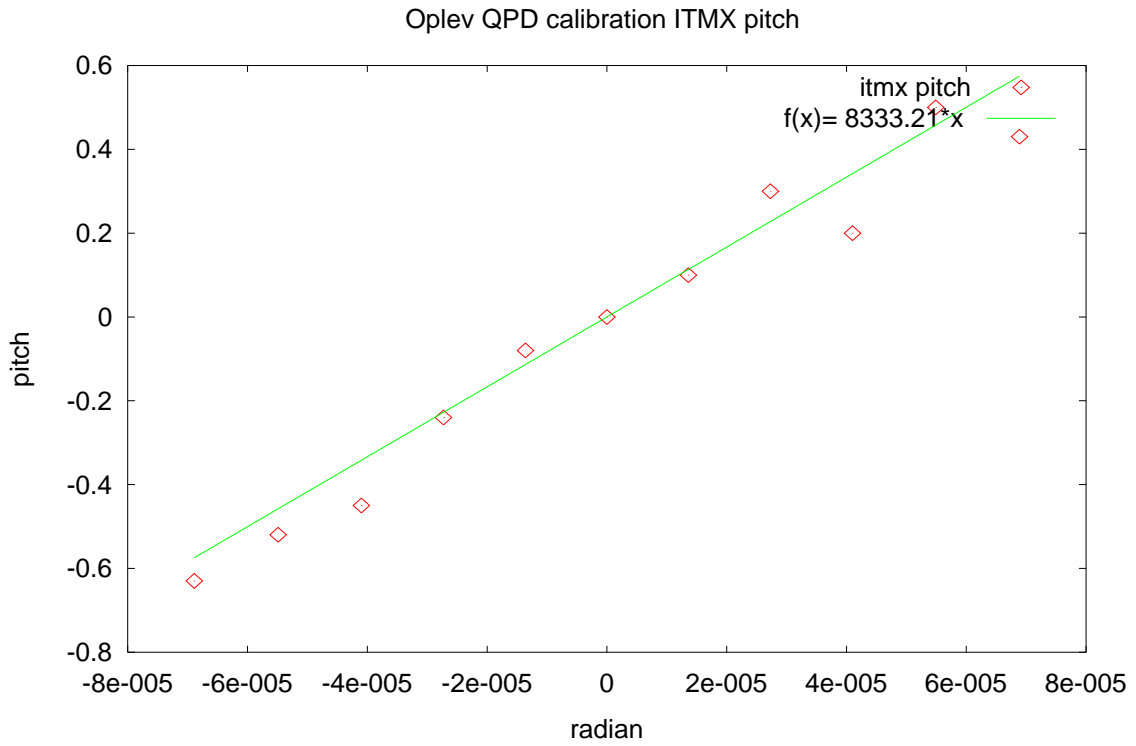


Fig. 12: ITMX pitch and yaw

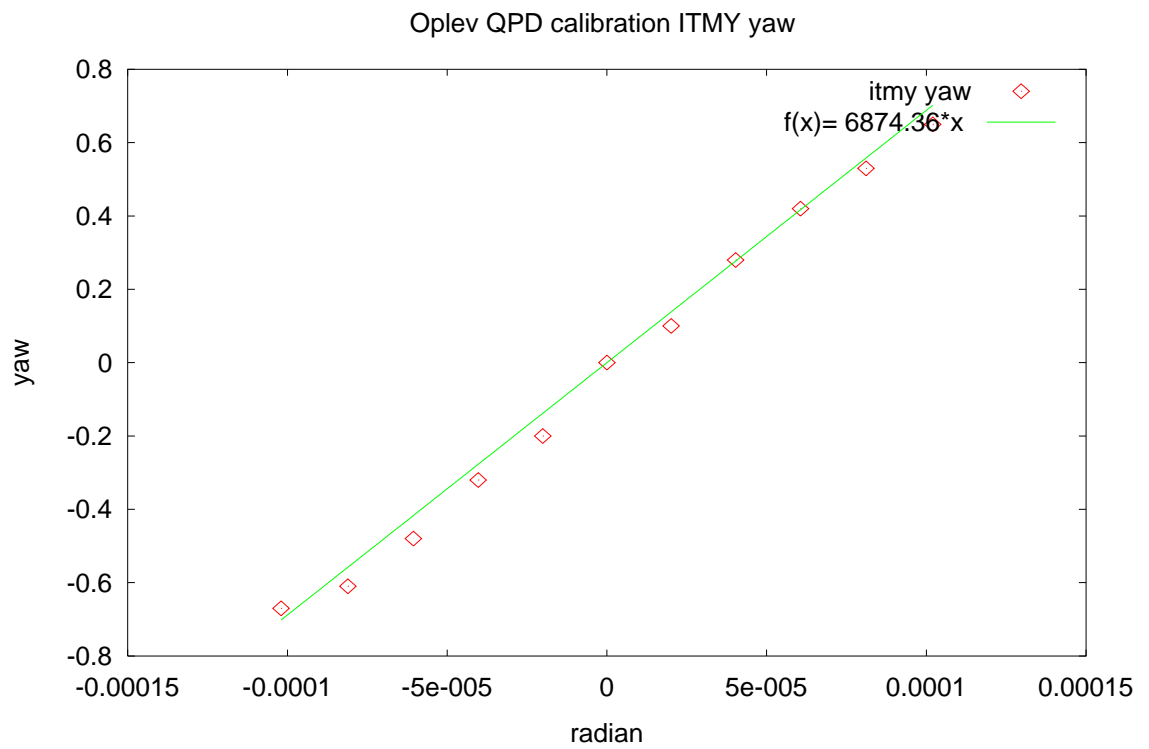
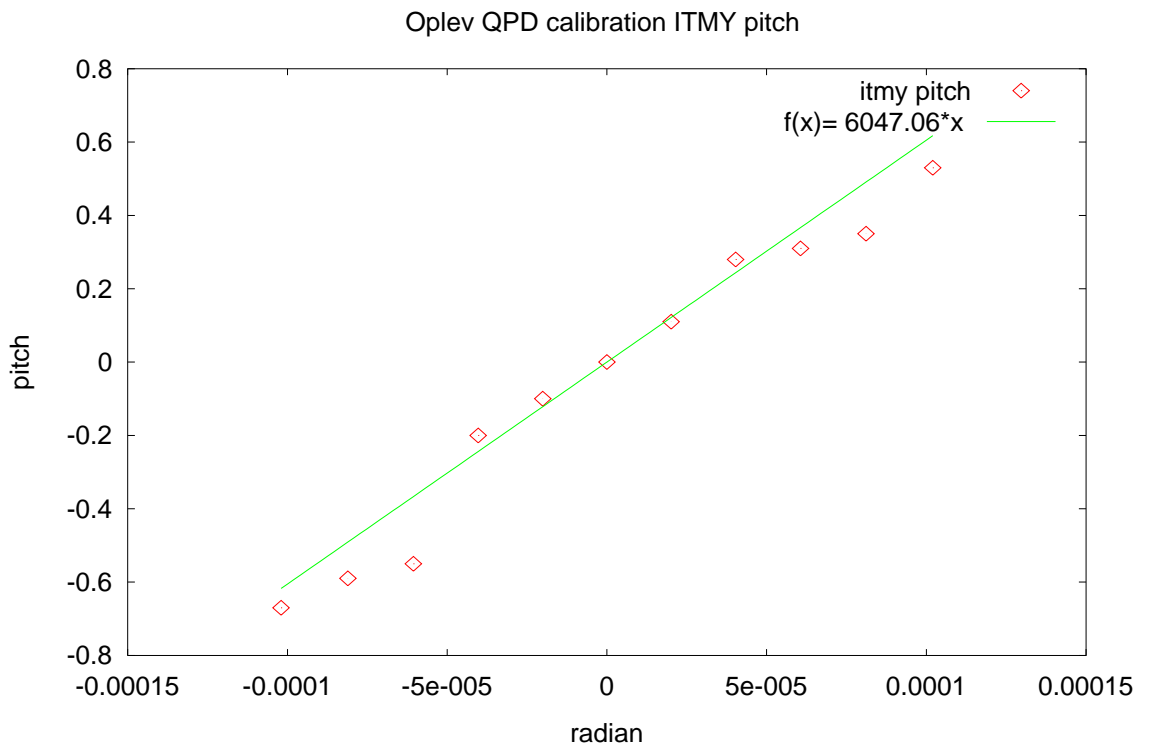


Fig. 13: ITMY pitch and yaw

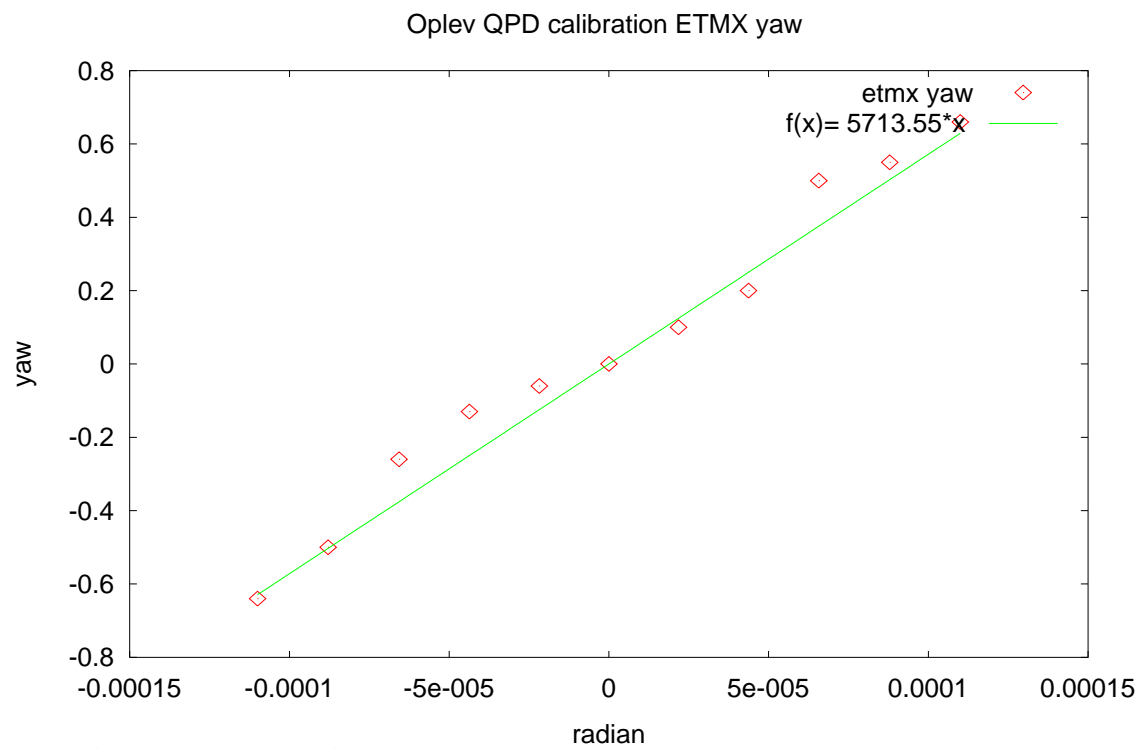
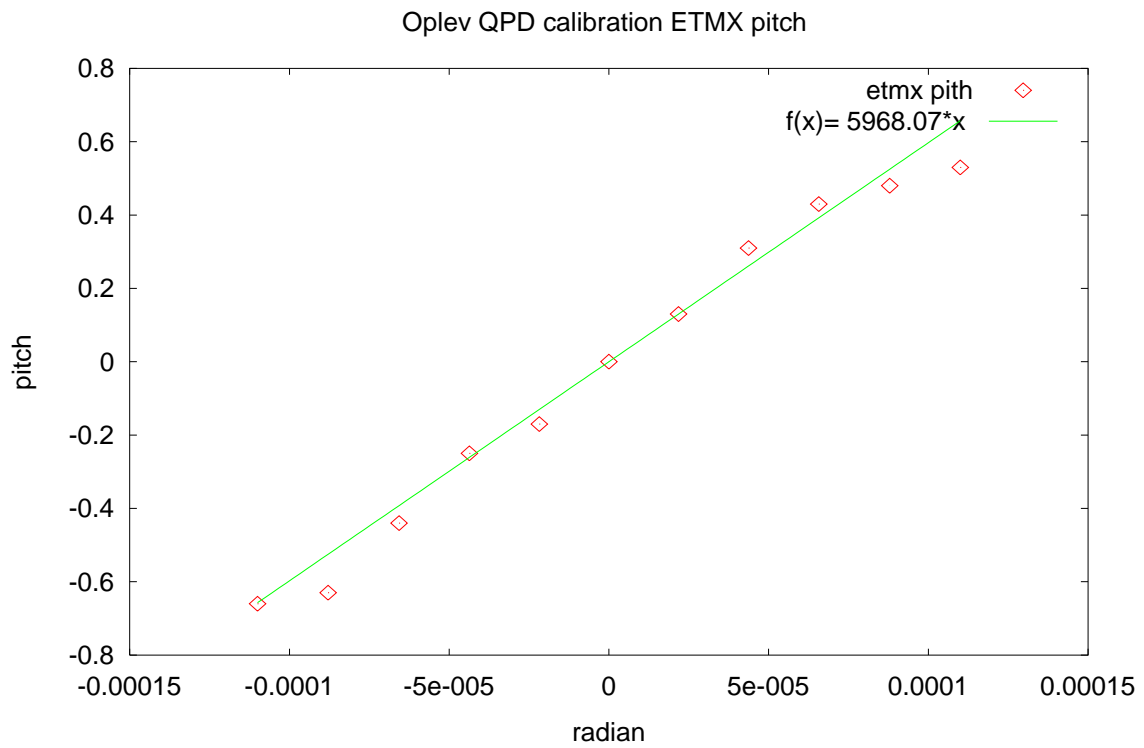


Fig. 14: ETMX pitch and yaw

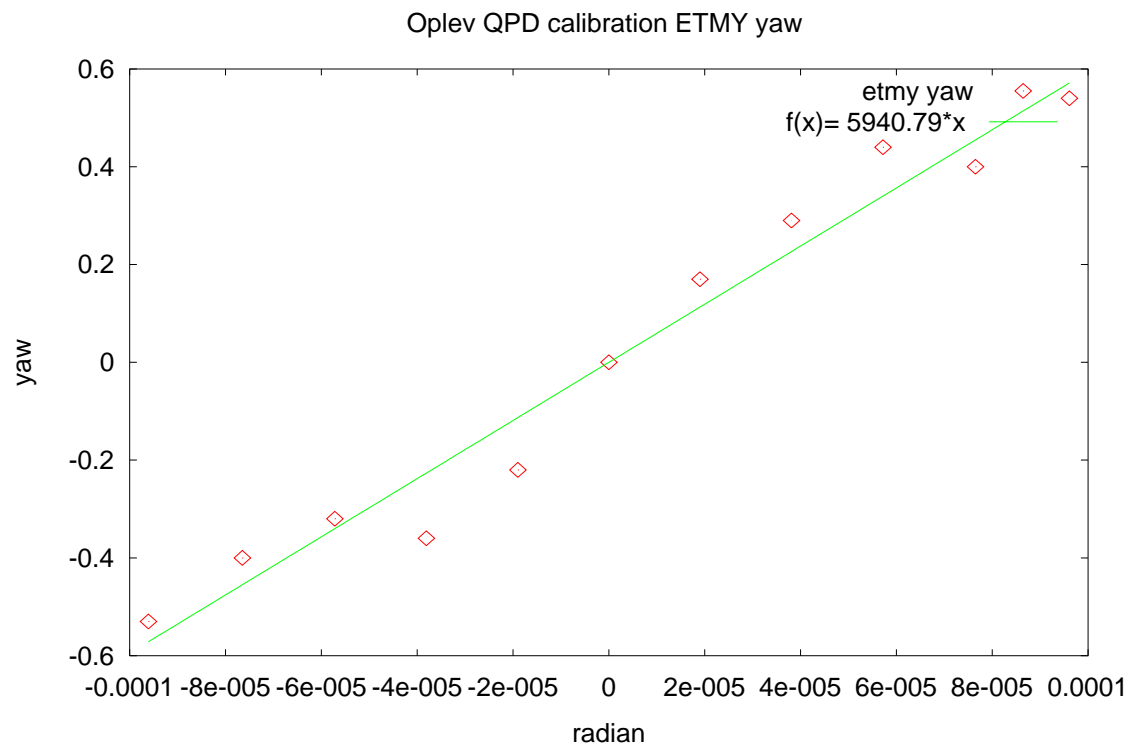
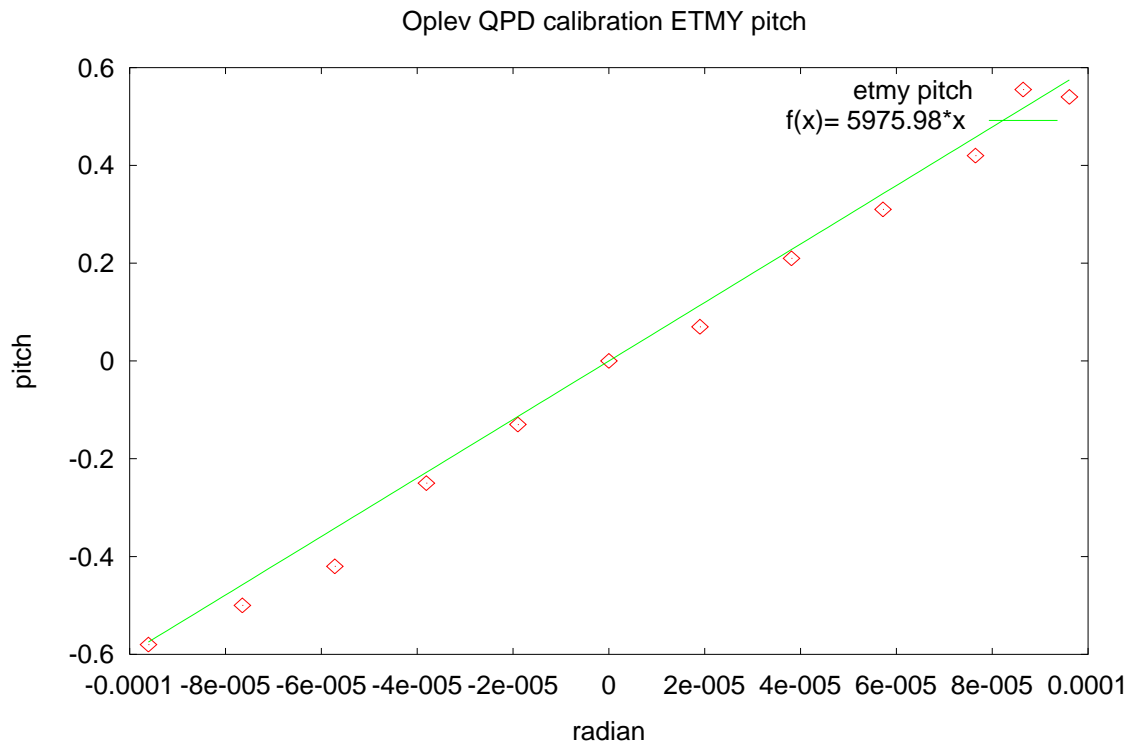


Fig. 15: ETMY pitch and yaw

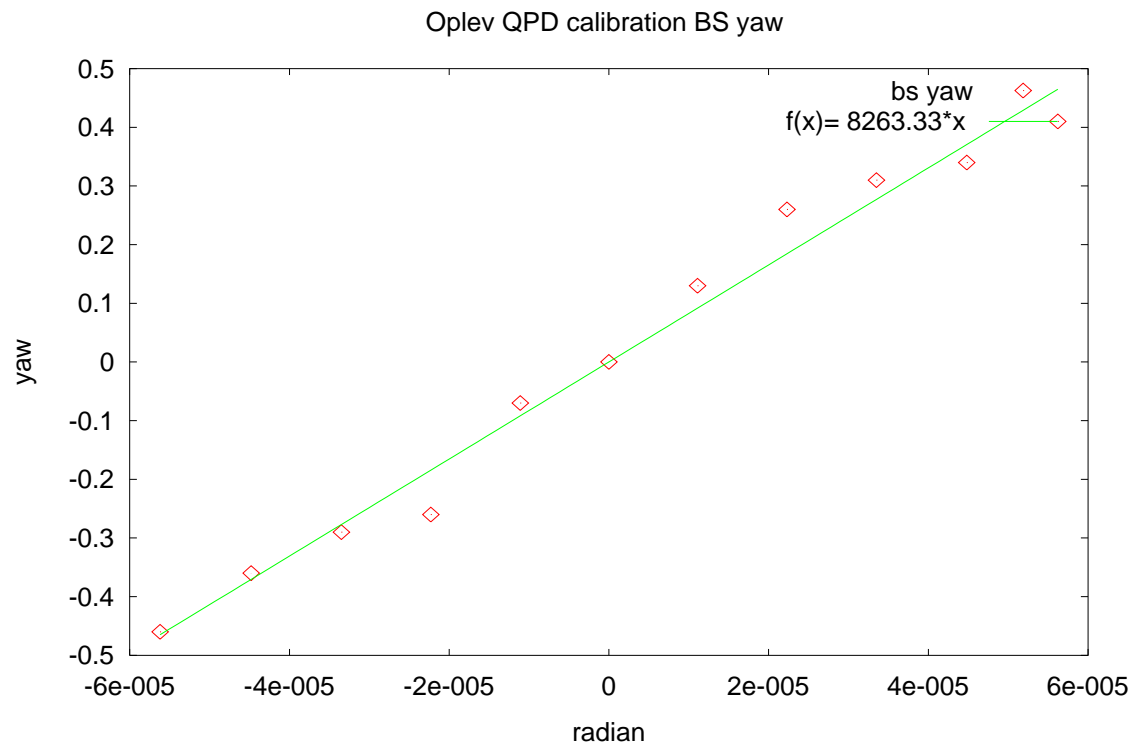
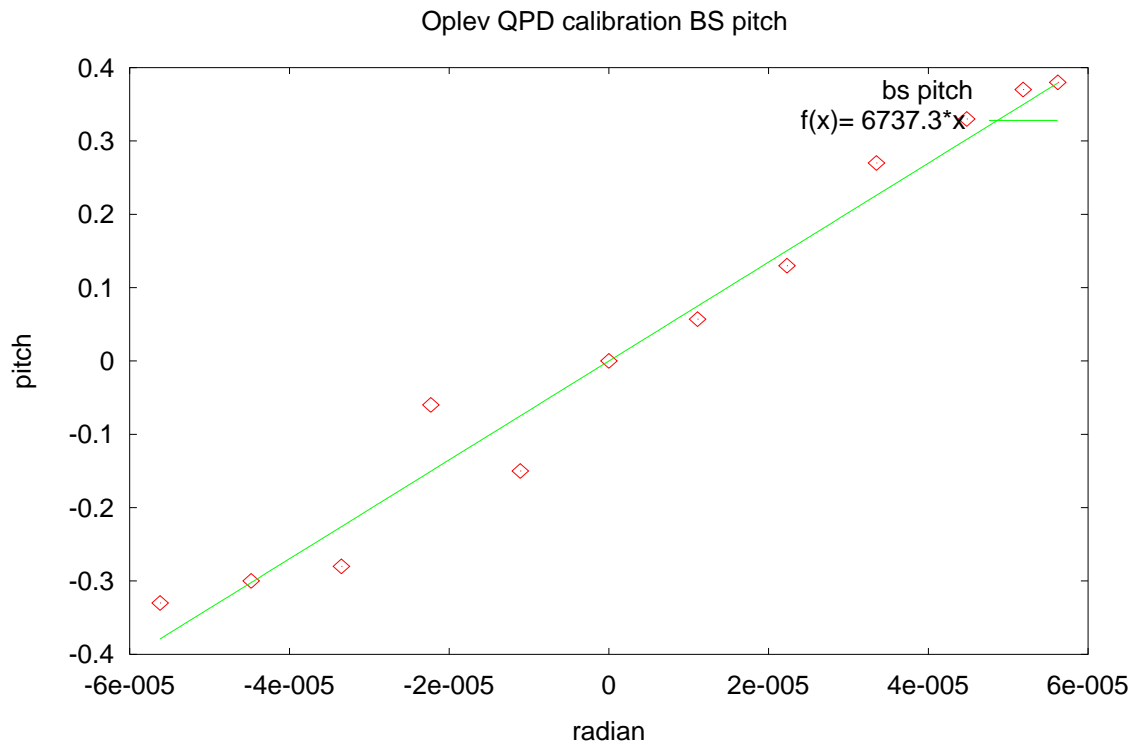


Fig. 16: BS pitch and yaw

The calculated calibration factors are listed below.

Optic	R(cm)	Pitch calibration factor c (arbitrary unit/radian)	Yaw calibration factor c (arbitrary unit/radian)
ITMX	270.2	8333	7272
ITMY	167.5	6047	6874
ETMX	181.9	5968	5714
ETMY	192.8	5976	5941
BS	363.9	6737	8263

Chart 2: Calculated calibration factors of the 5 optics. Here R is a distance from an optic to a QPD, or returning beam length.

3 Optical lever system sensitivity

In order to use the Oplev signals as input to a feedback servo on the optics to stabilize their angular motion it is essential to determine the frequency region where the sensitivity of the Oplev system is sufficiently sensitive so that the feedback can be properly applied to the system. In order to verify that the Oplev signals contain the information of the optics angular motion, noise characterization was done.

3.1 Expected noise sources in the system

There are several possible noise sources in the Oplev system. Noise sources appear in the output of the system which will be fed back to control the optics. There are three main expected noise sources in the system: seismic noise, beam jitter noise, and electronic noise.

Because the Oplev system is on optical tables which do not have seismic attenuation systems, the seismic noise in the Oplev systems are expected to be larger than that of the table on which the optics are placed.

The beam jitter noise from the 670nm lasers is expected to be relatively large due to the quality of the lasers.

The electronic noise comes into the system from various places and is expected to dominate at the higher frequencies.

As attempts to measure each of these noises were made, it turned out that the beam jitter noise and the seismic noise are difficult to separate from the signal due to too many uncertainties in the measurements: (e.g. the optical table for BS Oplev is on the additional plate which is placed on the floor, making the table shake differently than other tables, but BS optical table is the one which is able to be used for the measurement.)

3.2 Noise characterization

Although it is difficult to measure each of the noise sources at the moment, it is possible to measure the total noise and search the frequency region where it is dominated by the noise due to the angular motion of the optics.

When it is assumed that the optical tables follow the seismic movement at lower frequencies, the RMS noise of the tables can be expressed as the typical RMS spectrum of seismic noise which can be approximated to $S = \frac{10^{-7}}{f^2} [m / \sqrt{Hz}]$

The RMS noise of the optics motion caused by the ground motion can be approximated by applying transfer functions of the seismic stacks and the transfer function of the pendulum to the spectrum of the seismic noise. The stacks' transfer functions and the damped pendulum transfer function can be written as

$$H = Abs \left[\frac{\omega_i^2 + j \frac{\omega_i \omega}{Q_i}}{\omega_i^2 + j \frac{\omega_i \omega}{Q_i} - \omega^2} \right] \text{ here, the subscript } (i = s1, s2, s3, p) \text{ is used to represent}$$

the three stack modes (mode 1, 2, and 3) and the pendulum respectively. Their Q factors and resonant frequencies are listed below in chart 3.

	Resonant frequency	Typical Q-factor
Pendulum yaw	0.5	10
Mode 1	8.5	4.2
Mode 2	22	4
Mode 3	40	4

Chart 3: Resonant frequencies and the typical Q-factors of the pendulum and the three stack modes

The prediction for a typical seismic spectrum and the optics motion spectrum are plotted in Fig. 17.

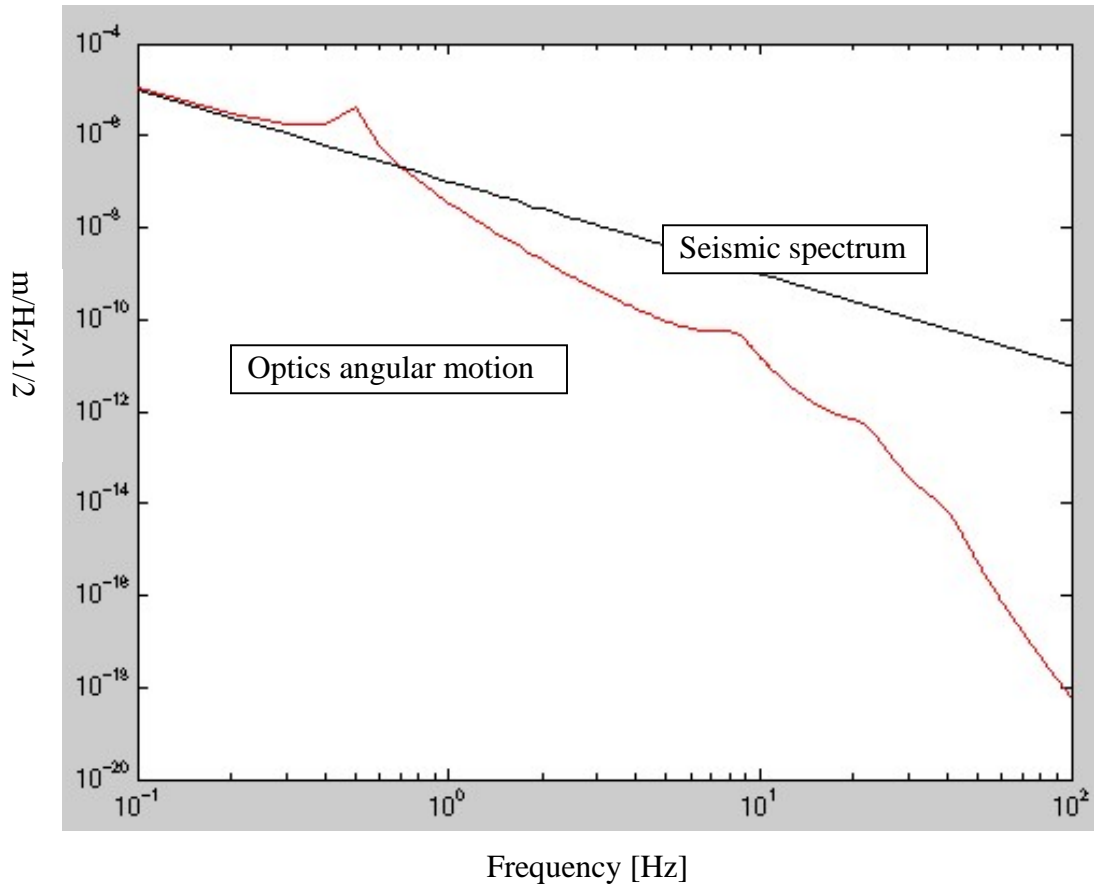


Fig. 17: Prediction for the spectra of the optics angular motion and the seismic noise

From Fig. 17 you can see that around the pendulum's resonant frequencies the motion of the optic can be detected above the seismic noise which can then be fed back to control the optics.

The noise was also measured to verify that the signal from the optics' angular motion dominates over the total noise at the resonant frequency. The noise was measured with two settings: one with the beam hitting the optic and the other without the beam hitting the optic. Comparing these should tell if the signal due to the optic's motion dominates at its resonant frequency. Fig. 18 shows the two settings. Here ETMY was selected because it has enough space on the optical table for the measurement.

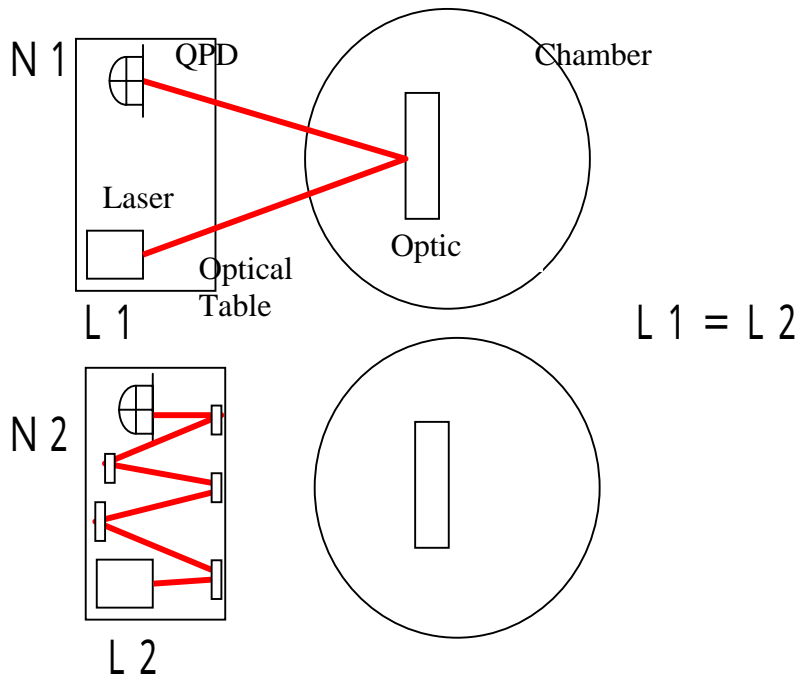


Fig. 18: Set up of the noise measurement: one with the beam hitting the optic and the other not hitting it.

The noise spectra of yaw and pitch were taken from C1:SUS-ETMY_OLPIT/YAW_IN1. The beam paths are the same for both settings of the measurement. ($L_1=L_2=347.2\text{cm}$). The spectra are shown in Fig. 19 below.

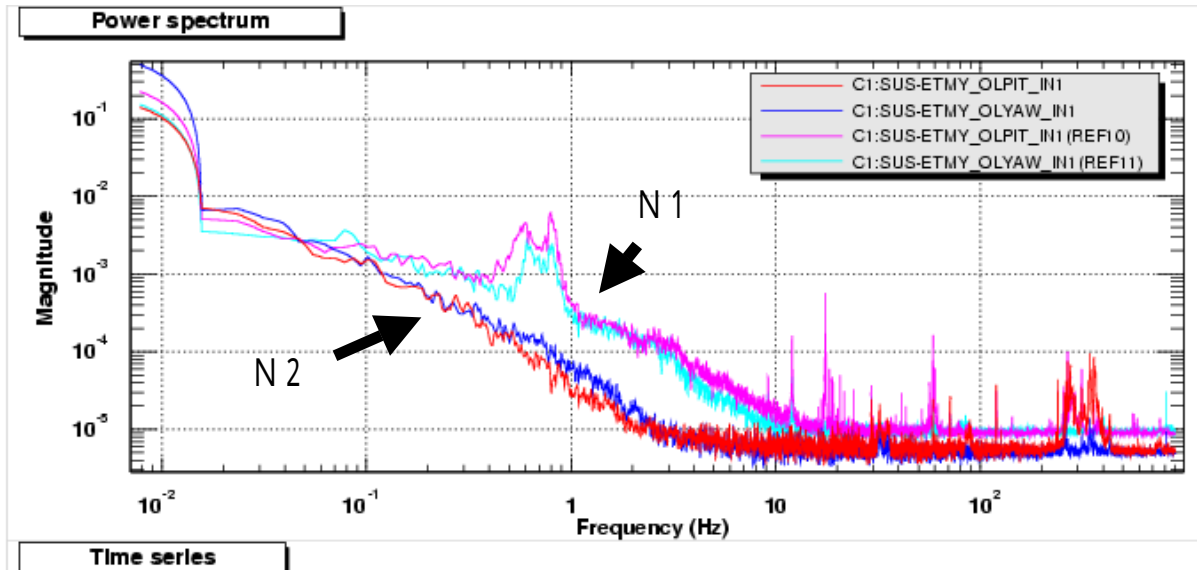


Fig. 19: Noise power spectra of pitch and yaw

N1 includes the noise from the optic while N2 does not. From the figure it can be concluded that in the frequency range between 0.1 and 10 Hz the optics motion dominates the total noise.

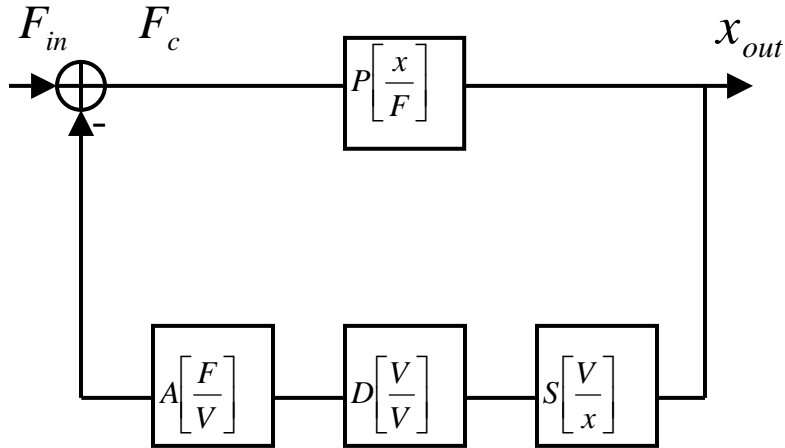
This result indicates that the optics can be controlled with proper feedback loop in the vicinities of the resonant frequency.

4 Controlling the optics

4.1 Q-factor

In order to control the optics to damp their motion around their resonant frequencies the Oplev signals have to be fed back on the optics through the control loop. Figure 20 shows the control loop of the system. It is a negative feedback loop. F_{in} is a force due to noise sources acting on a suspended optic and x_{out} is the motion of the optic. The goal is to make x_{out} small.

Without closing the feedback loop the force acting on the suspended optics will be amplified by the suspension resulting in a large motion of the optics at the suspension's resonant frequency.



P : transfer function of the suspended optic

S : transfer function of the sensor

D : transfer function of the digital filter

A : transfer function of the actuator

F : force

x : displacement

V : volts

Fig. 20 : Oplev control loop

When the loop is closed as shown in Fig. 20, x_{out} can be expressed as

$x_{out} = \frac{P}{1+G} F_{in}$ where the gain of the open loop transfer function $G = PSDA$. When $G \gg 1$ this becomes

$x_{out} = \frac{P}{G} F_{in} = \frac{1}{SDA} F_{in}$. By designing a proper digital filter D , x_{out} can be minimized

and the Q-factor can be changed. Fig. 21 explains how the Q-factor is changed. Figure 21-a shows the gain of the suspended optic's transfer function. It has a Q-factor of Q_0 . Figure 21-b shows the transfer function of the digital filter and Fig. 21-c shows the transfer function from F_c to the feedback signal (open-loop transfer function). Because

the transfer functions of the sensor and the actuator have flat magnitude response, the overall response of the open-loop transfer function is expressed as a product of the transfer functions of the suspended optic and the digital filter. Where the gain of the open-loop transfer function G is much larger than 1, with the control loop closed, the Q-factor of the suspended optic will be reduced inversely proportional to the gain of the open-loop transfer function, making $Q \approx \frac{Q_0}{G}$. The digital filter here is a high-pass filter with a zero at 0 Hz and two poles at 3 Hz.

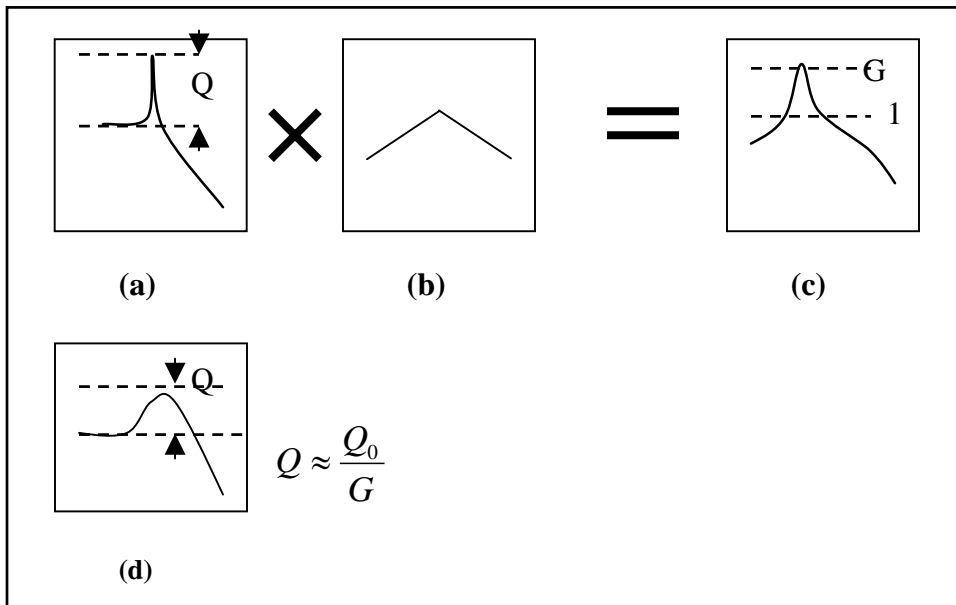


Fig. 21: Schematic diagram of the transfer functions. (a) shows the transfer function of the suspended optic when the control loop is open. (b) shows the transfer function of the digital filter. (c) shows the transfer function from F_c to the feedback signal. (d) shows the transfer function of the suspended optic when the control loop is closed.

Measuring the Q-factor of the damped optic will tell how well the optic is damped. The ideal case is when the optic is critically damped although trying to achieve critical damping by OSEM system is noted to cause noise at higher frequencies and this limits how much the OSEM system can damp the optics. Thus it is important to use Oplev system to help damp the optics. In order to see how much the Oplev system together with the OSEM with its typical value of gain can damp the optics, the Q-factor was measured with various values of the Oplev filter gain with a fixed OSEM gain which is typically used.

To observe the Oplev system damp the optics, the transfer function of the suspended optics are measured and the Q-factors were calculated using the software LISO.

As a result we observed the Oplev damp the optics close to critical damping (Q-factor of 0.5) as shown in Fig. 22. We conclude that with a proper modification to the filters the Oplev system can be used to help damp the optics motion at the resonant frequency. From Fig. 22 it seems that the value of the Q-factor decreases as the inverse square root of the value of the gain instead of as the inverse of the value of the gain. This is because the damping is caused not only by the Oplev system but also by the OSEM system, and when the gain of these two systems are comparable the rate of contribution of the Oplev gain to the system will be decreased and the slope will be gentler.

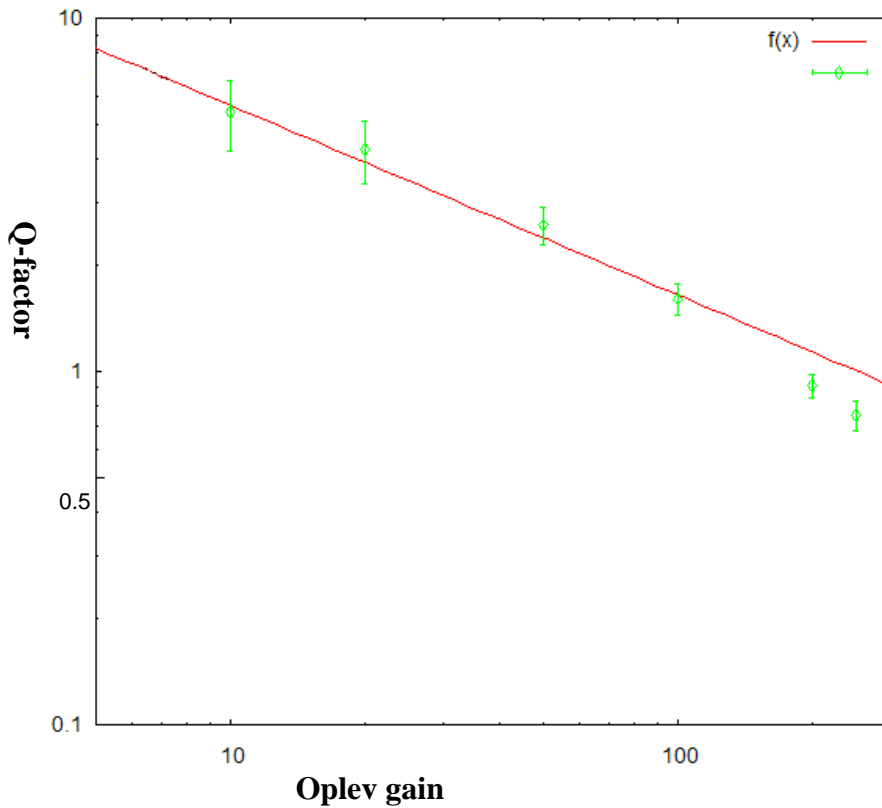


Fig. 22: Relationship between the Q-factor and the Oplev gain. When the system is critically damped the gain is 0.5.

4.2 Designing digital filters for Optical lever control loop

In order to reduce the angular motion at the pitch and yaw resonant frequencies and make it possible to help control the optics by the Oplev system, digital filters for each of the seven optics was designed using the software Foton. Each optic has the filters listed below in Chart 4. The high-pass filter has a zero at 0 Hz and two poles at 100 Hz. The resonant gains are placed at position resonant frequencies because there are strong couplings with position and pitch or yaw motion and motion at position resonant frequency tends to be larger.

		Zero (Hz)	Pole (Hz)	Resonant gain (Hz:Q:dB)
ITMX	Pitch	0	100,100	(0.8:5.3:40)
	Yaw	0	100,100	(0.8:5.3:30)
ITMY	Pitch	0	100,100	(0.8:4:14)
	Yaw	0	100,100	(0.8:2:10)
ETMX	Pitch	0	100,100	(0.8:3.2:20)
	Yaw	0	100,100	(0.8:5:20)
ETMY	Pitch	0	100,100	(0.8:8:26)
	Yaw	0	100,100	(0.8:4:20)
BS	Pitch	0	100,100	(1:10:30)
	Yaw	0	100,100	(1:10:30)
PRM	Pitch	0	100,100	
	Yaw	0	100,100	
SRM	Pitch	0	100,100	
	Yaw	0	100,100	

Chart 4: Oplev filters

(*during the process of designing and implementing the filters it was discovered that although the EPCS screen shows that the sampling rate of the Oplev servo is 16384Hz, it actually is 2048 Hz, thus when making digital filters a sampling rate of 2048 Hz should be selected on Foton.)

4.3 In-loop noise measurement

All the optics noises were measured from the port (C1: SUS-opticsname_OLPIT/YAW_IN1) when the feedback loop is on /off. It reads the OSEM sensor signal. The gain of the filters are set in such a way that it gives enough damping performance but small enough that it does not cause the oscillation in the system. The gain of the OSEM control loop is optimally set previously.

4.4 The result

The results are shown in Fig.23 through Fig.36. The blue is with Oplev servo off and the red is with Oplev servo on.

We observed that with the control loop on all the optics are well damped.

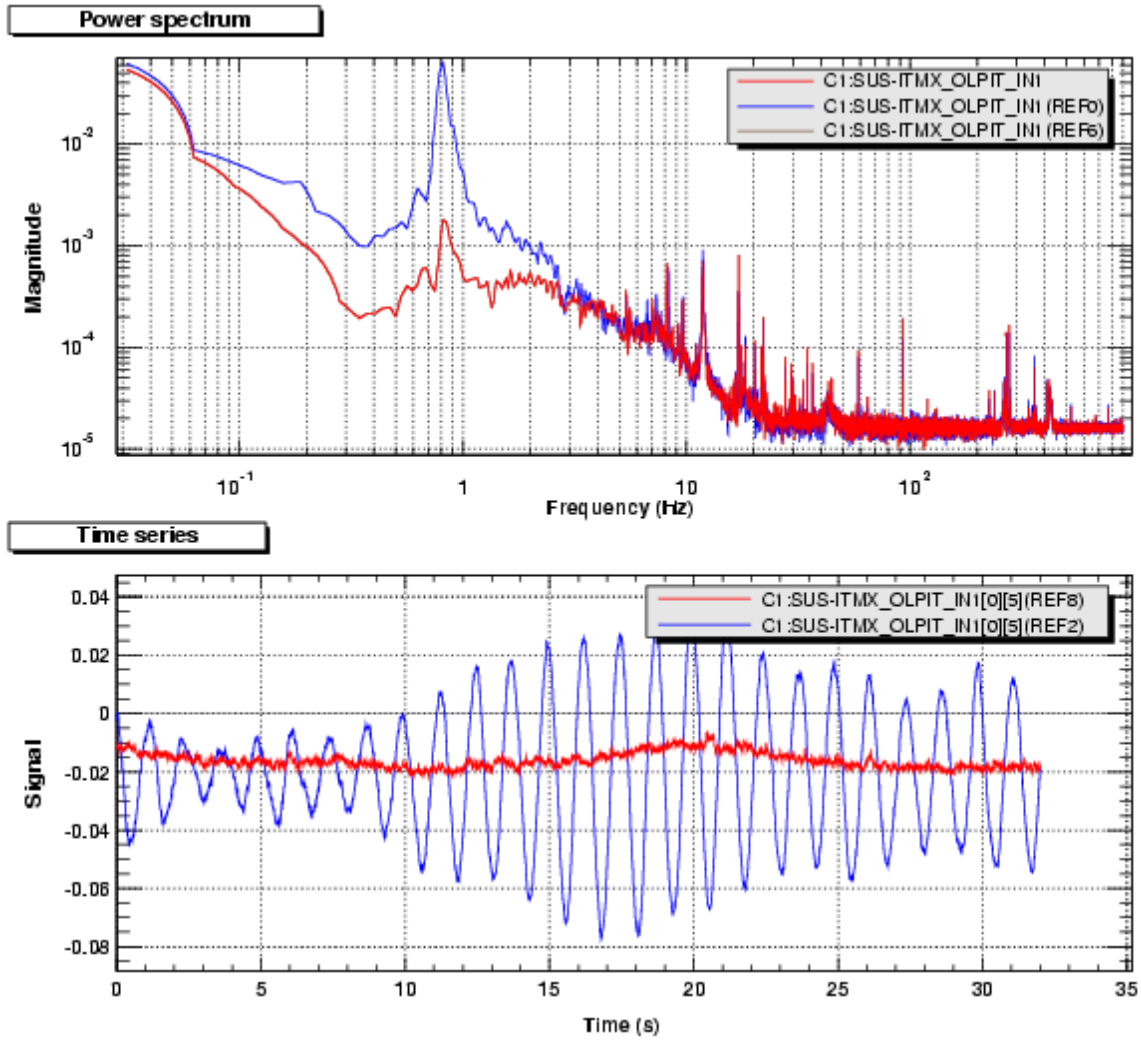


Fig. 23: In-loop noise spectra of ITMX pitch

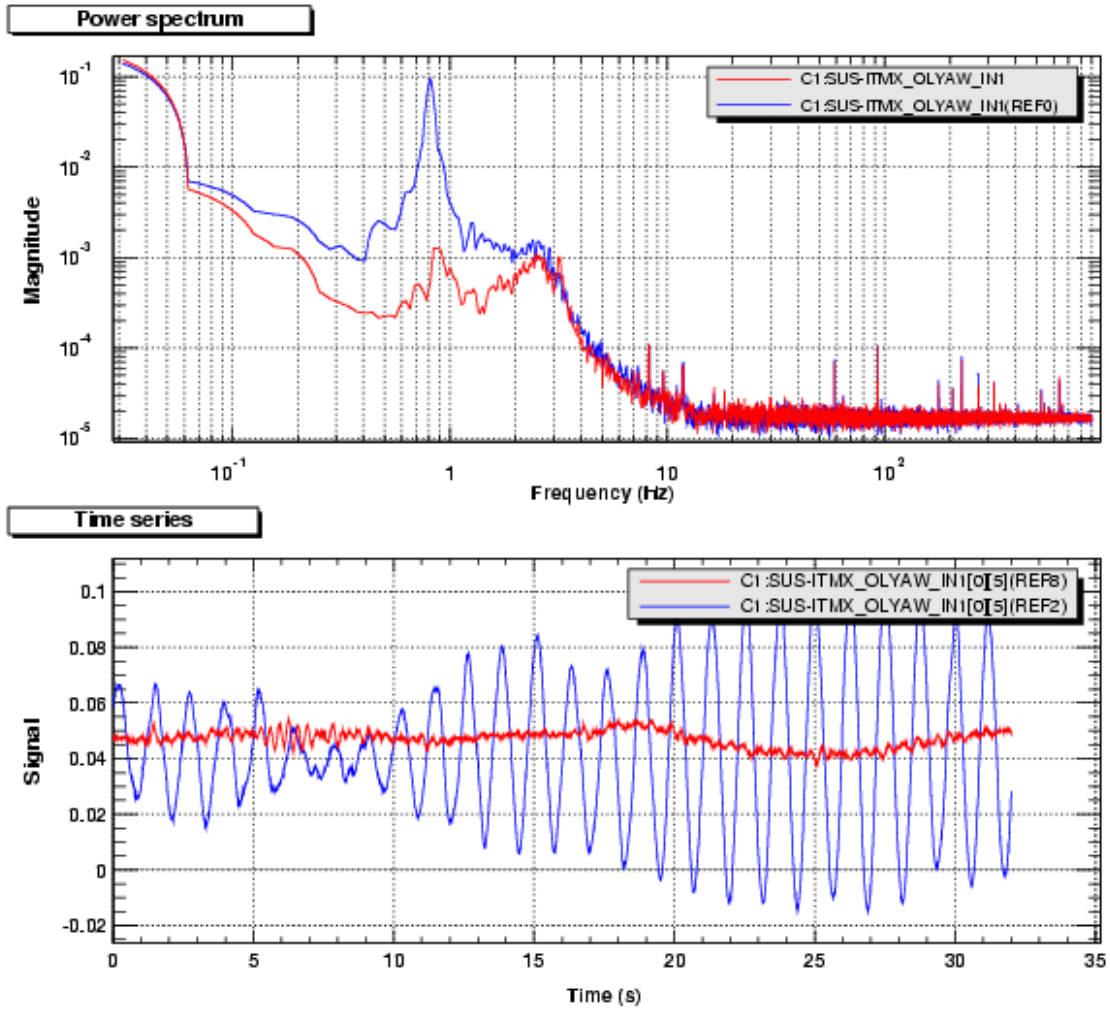


Fig. 24: In-loop noise spectra of ITMX yaw

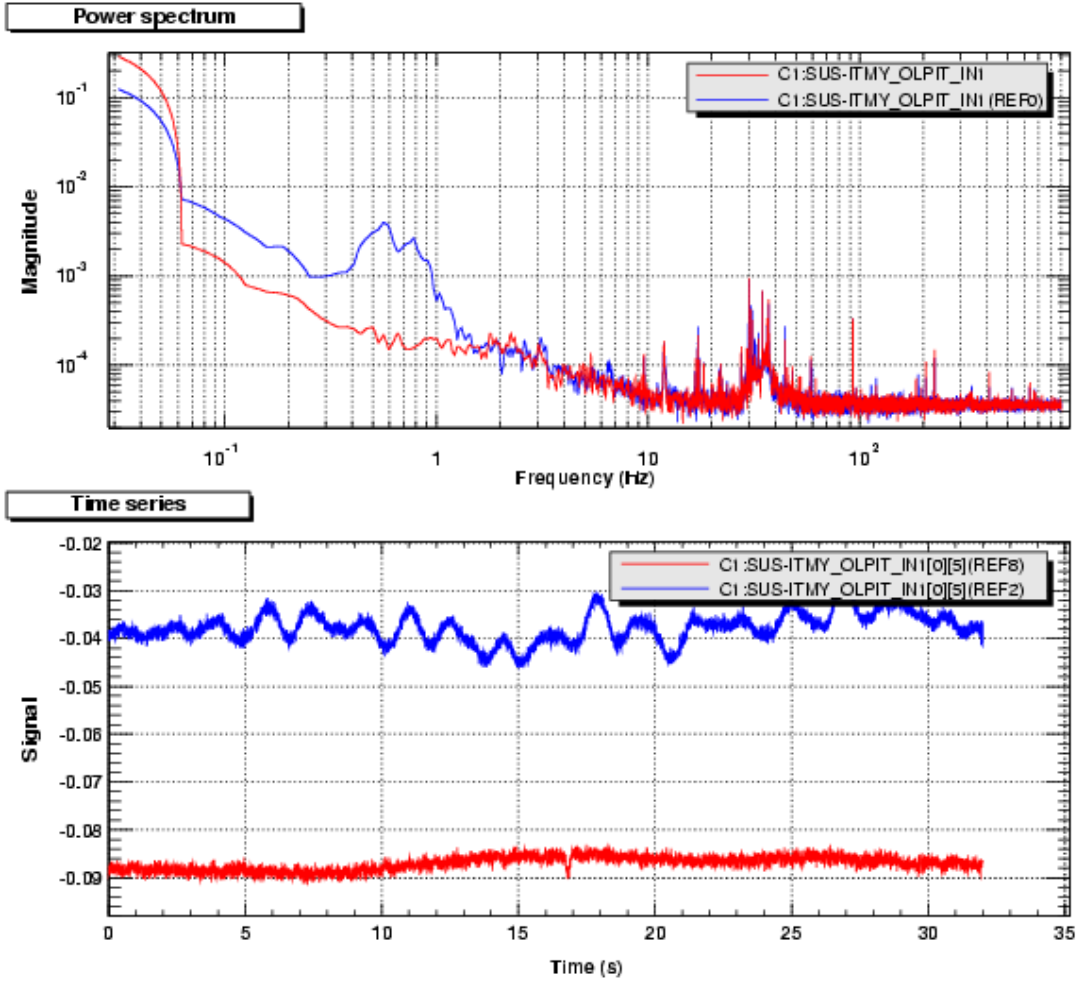


Fig. 25: In-loop noise spectra of ITMY pitch

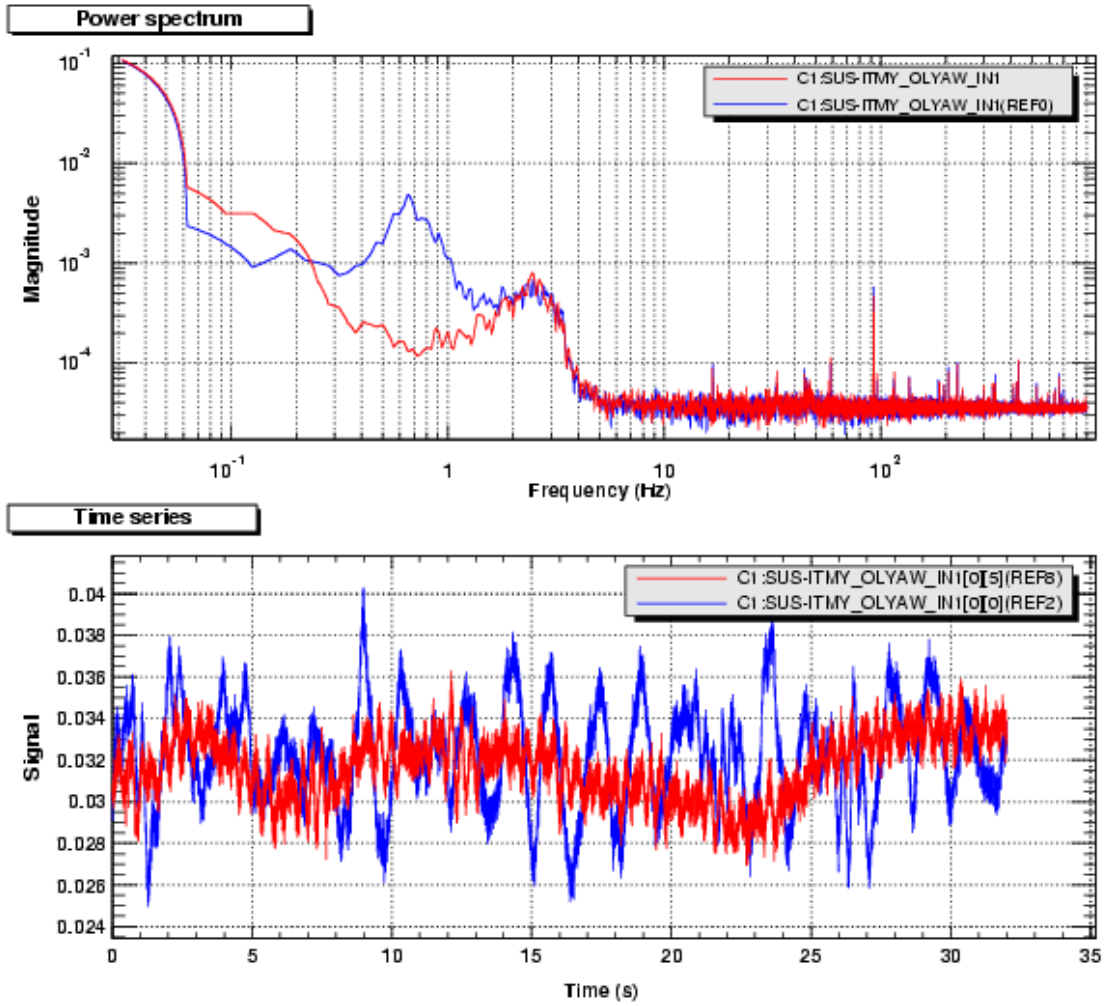


Fig. 26: In-loop noise spectra of ITMY yaw

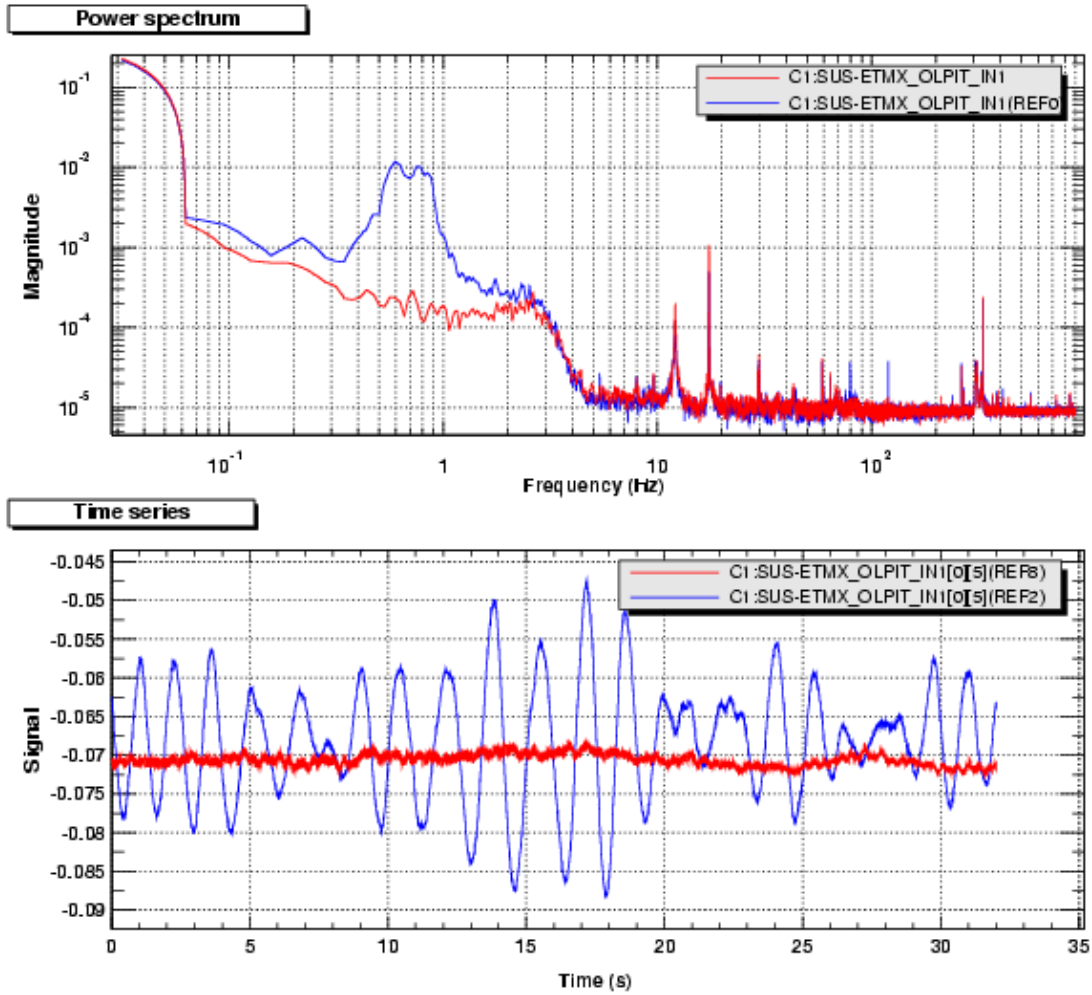


Fig. 27: In-loop noise spectra of ETMX pitch

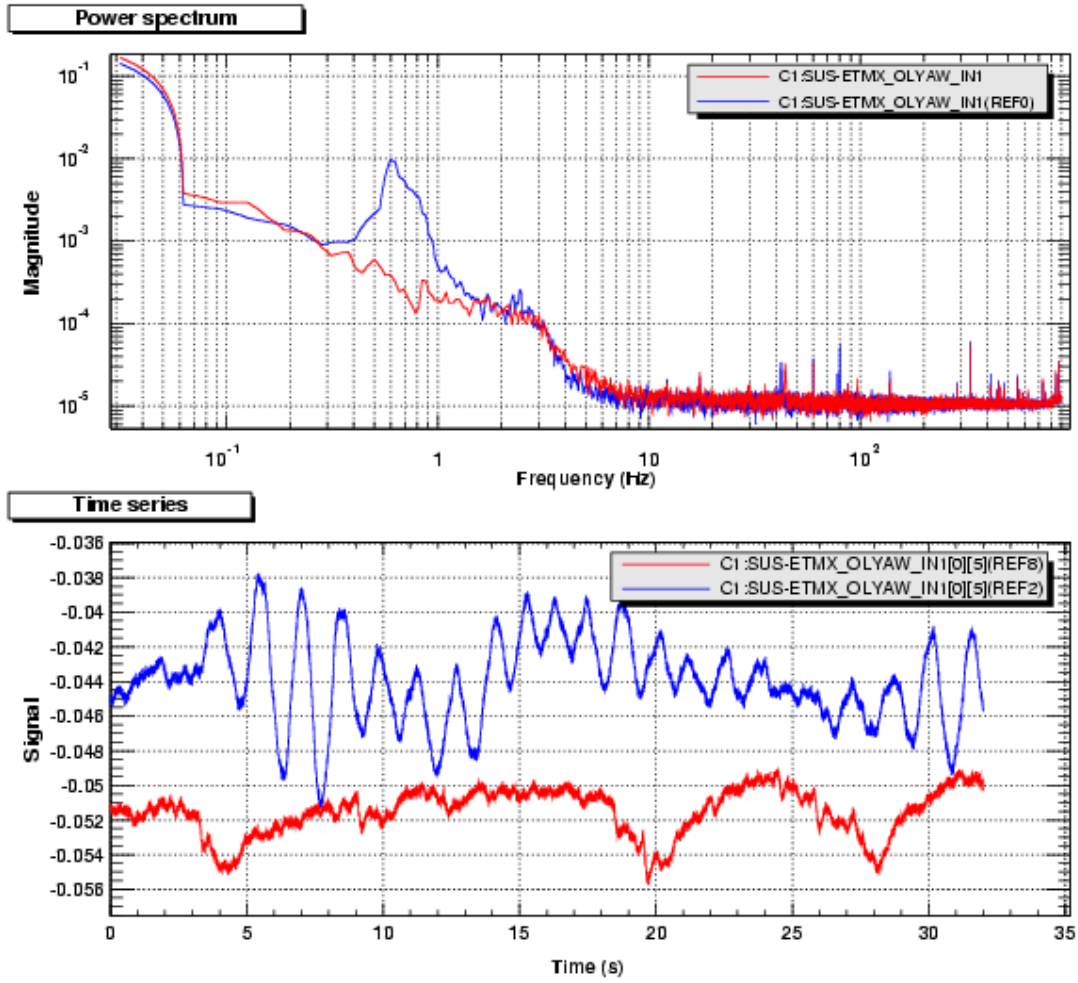


Fig. 28: In-loop noise spectra of ETMX yaw

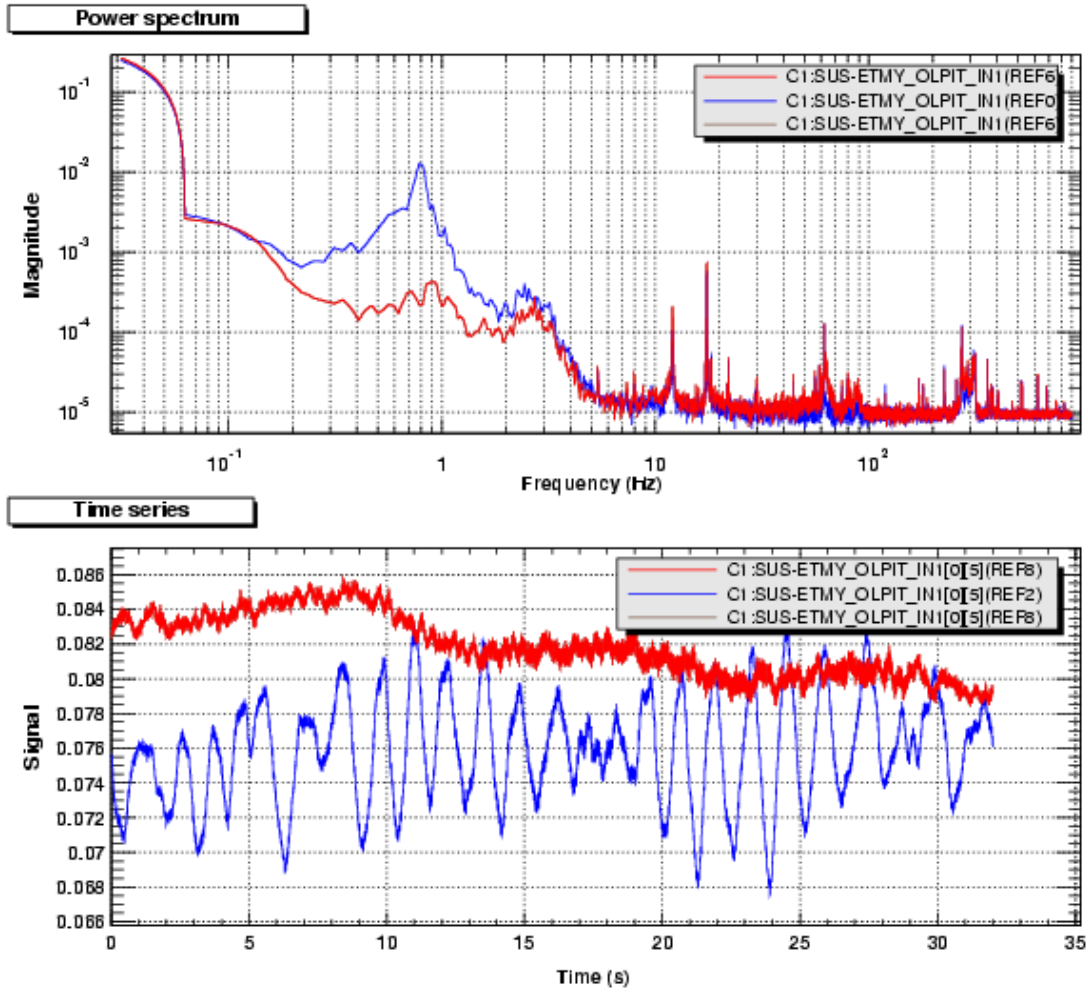


Fig. 29: In-loop noise spectra of ETMY pitch

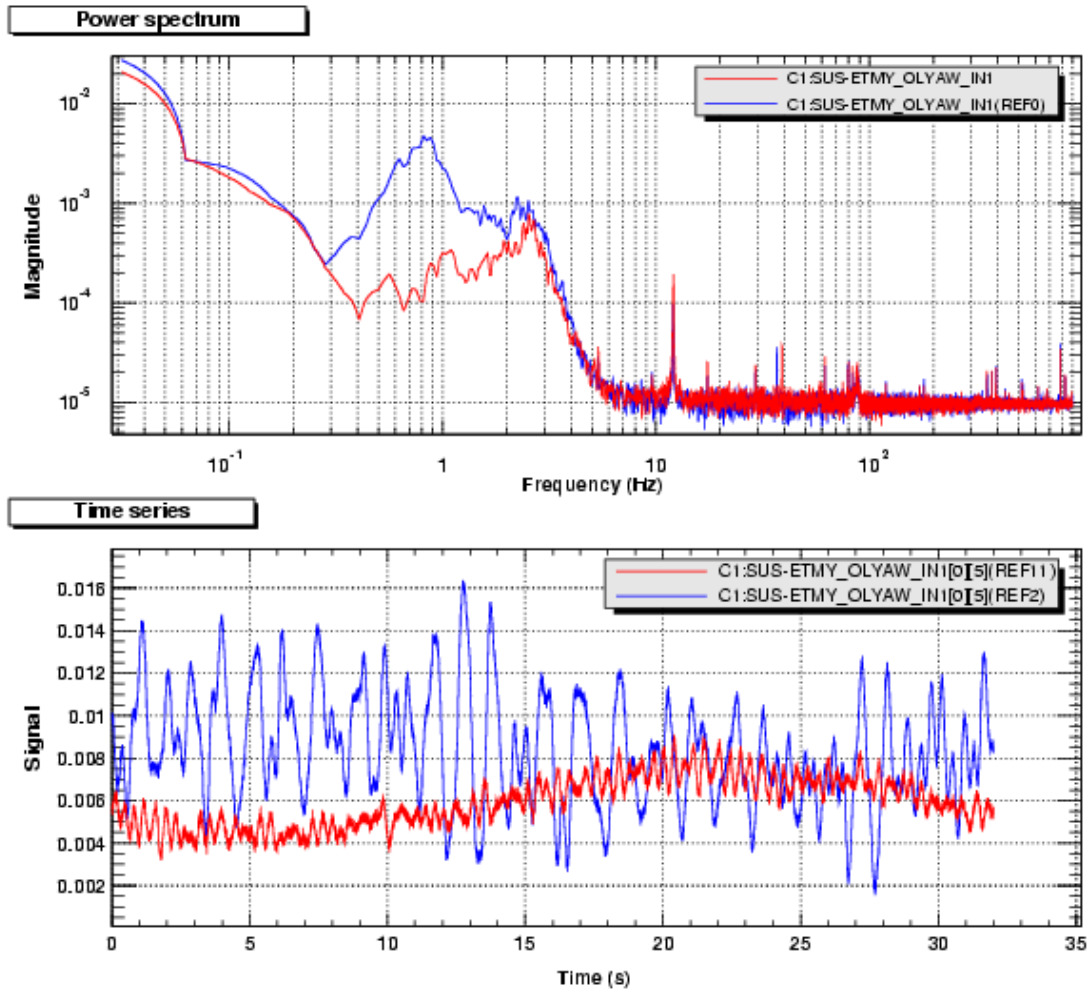


Fig. 30: In-loop noise spectra of ETMY yaw

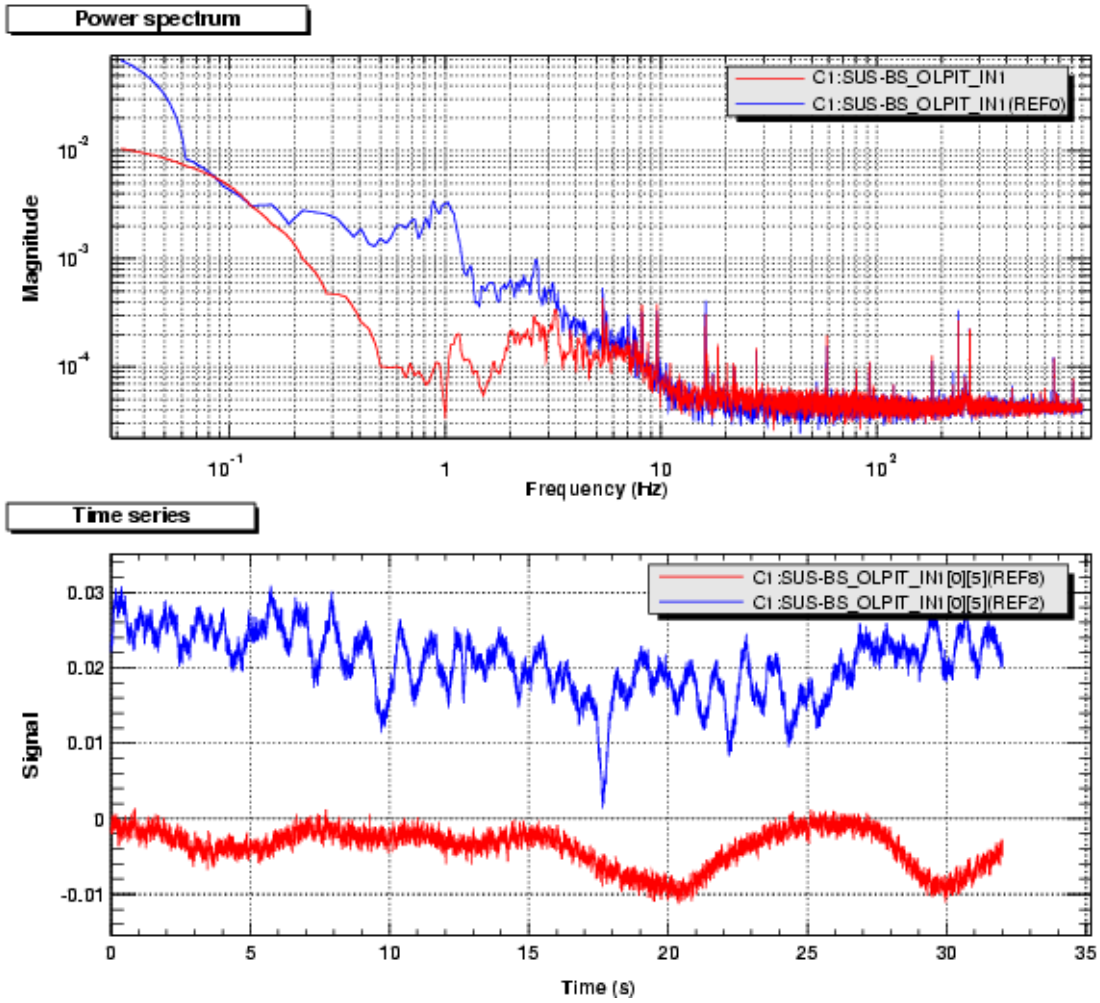


Fig. 31: In-loop noise spectra of BS pitch

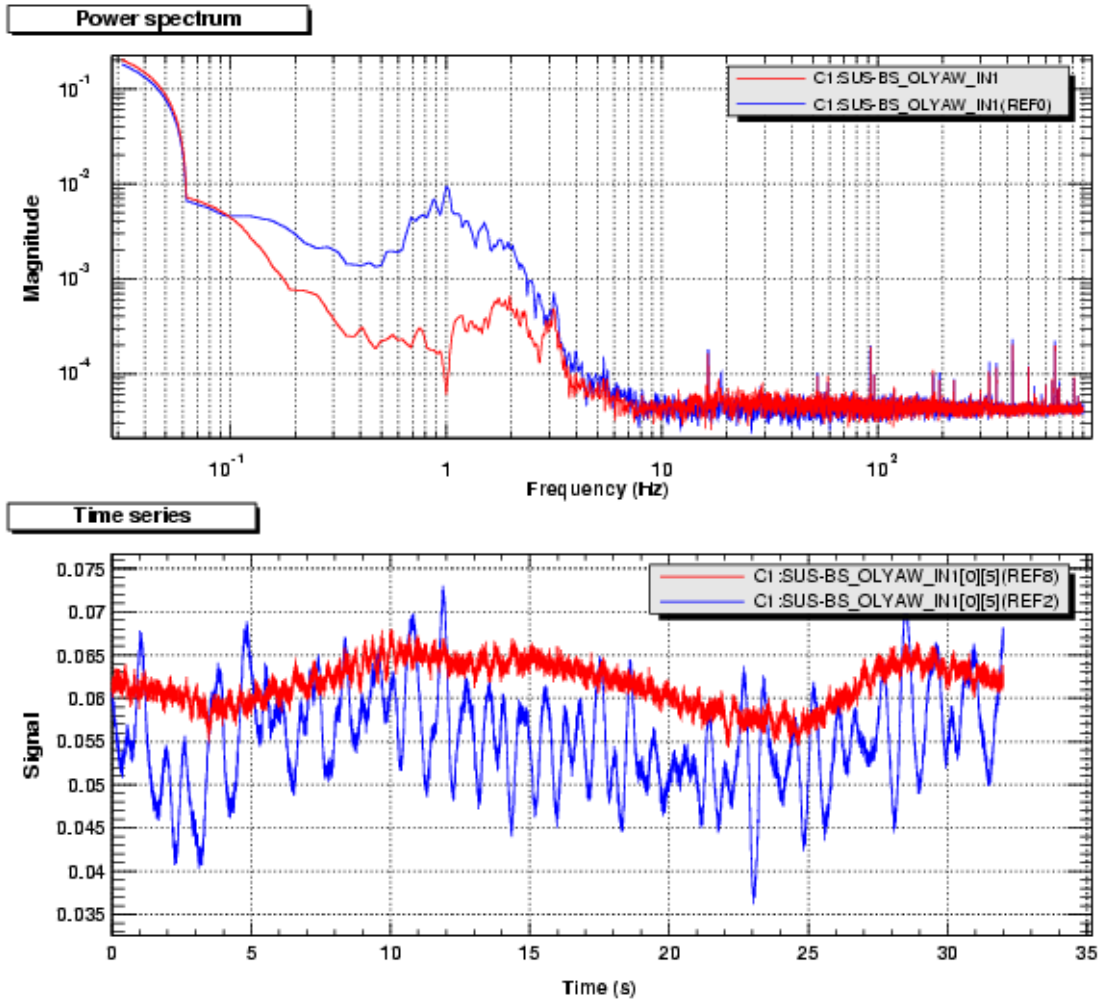


Fig. 32: In-loop noise spectra of BS yaw

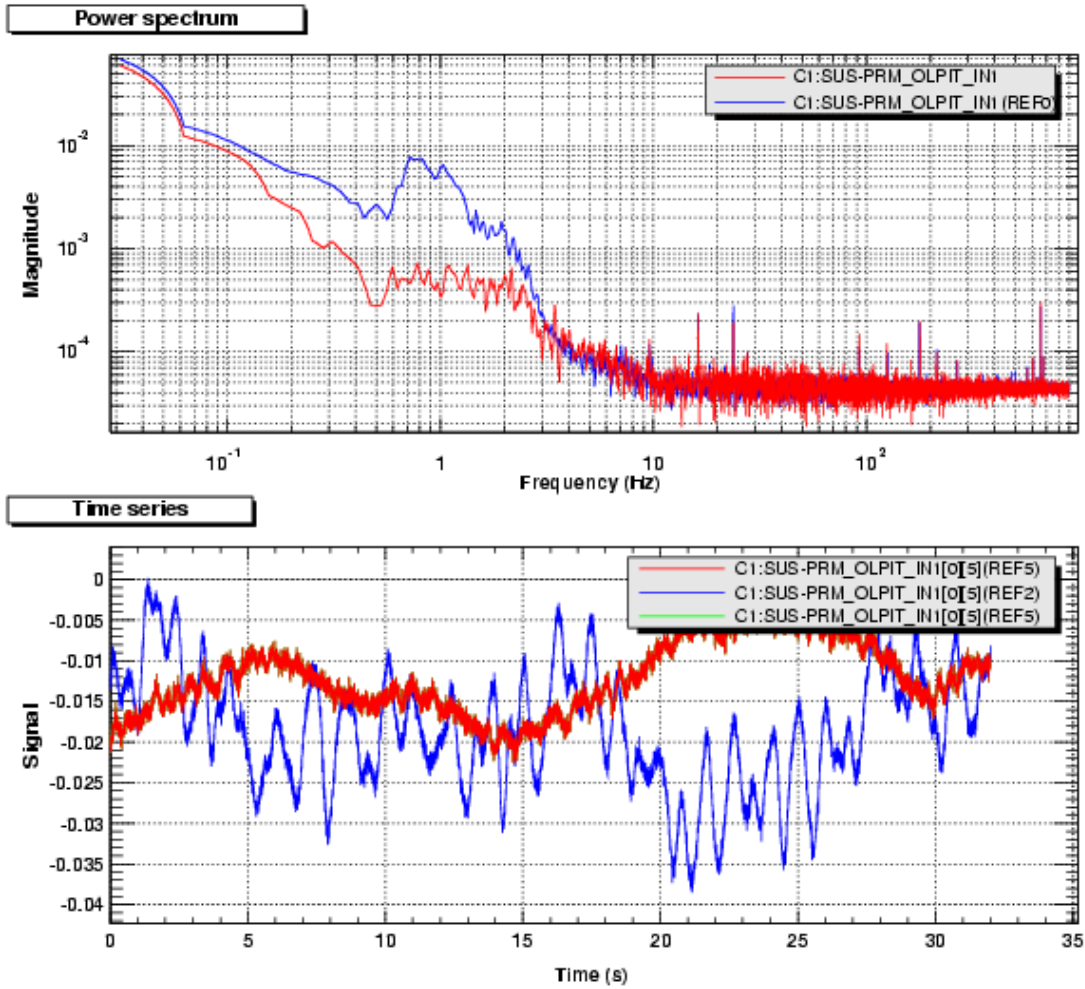


Fig. 33: In-loop noise spectra of PRM pitch

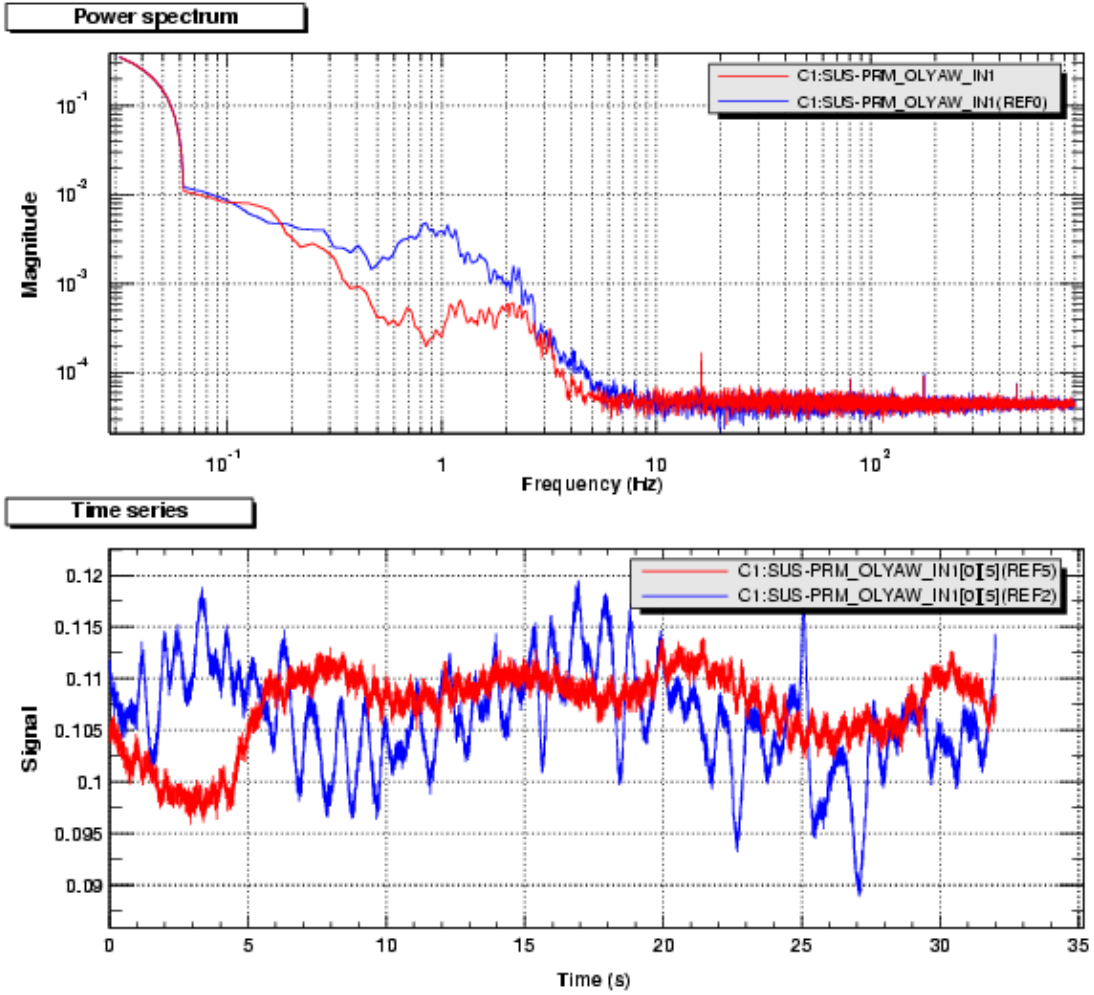


Fig. 34: In-loop noise spectra of PRM yaw

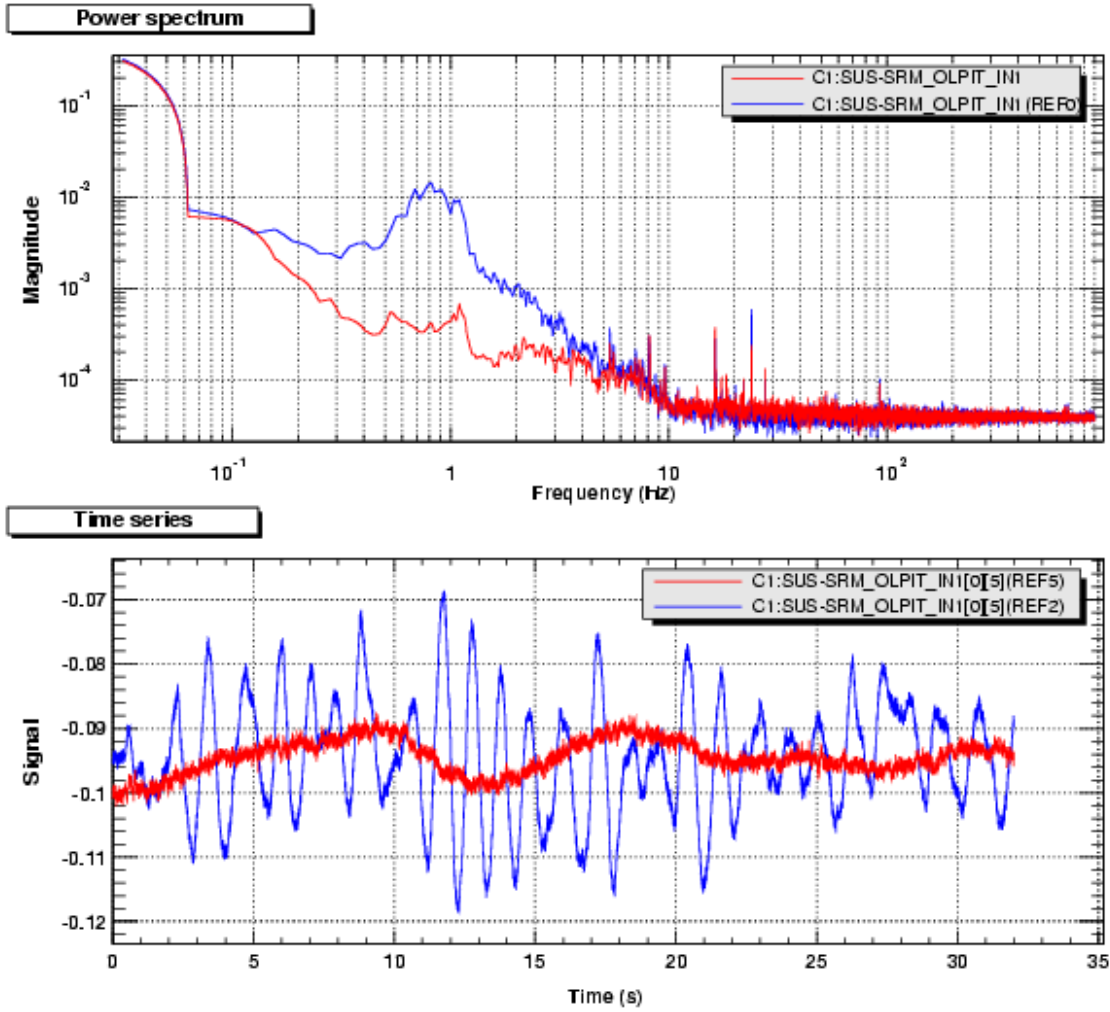


Fig. 35: In-loop noise spectra of SRM pitch

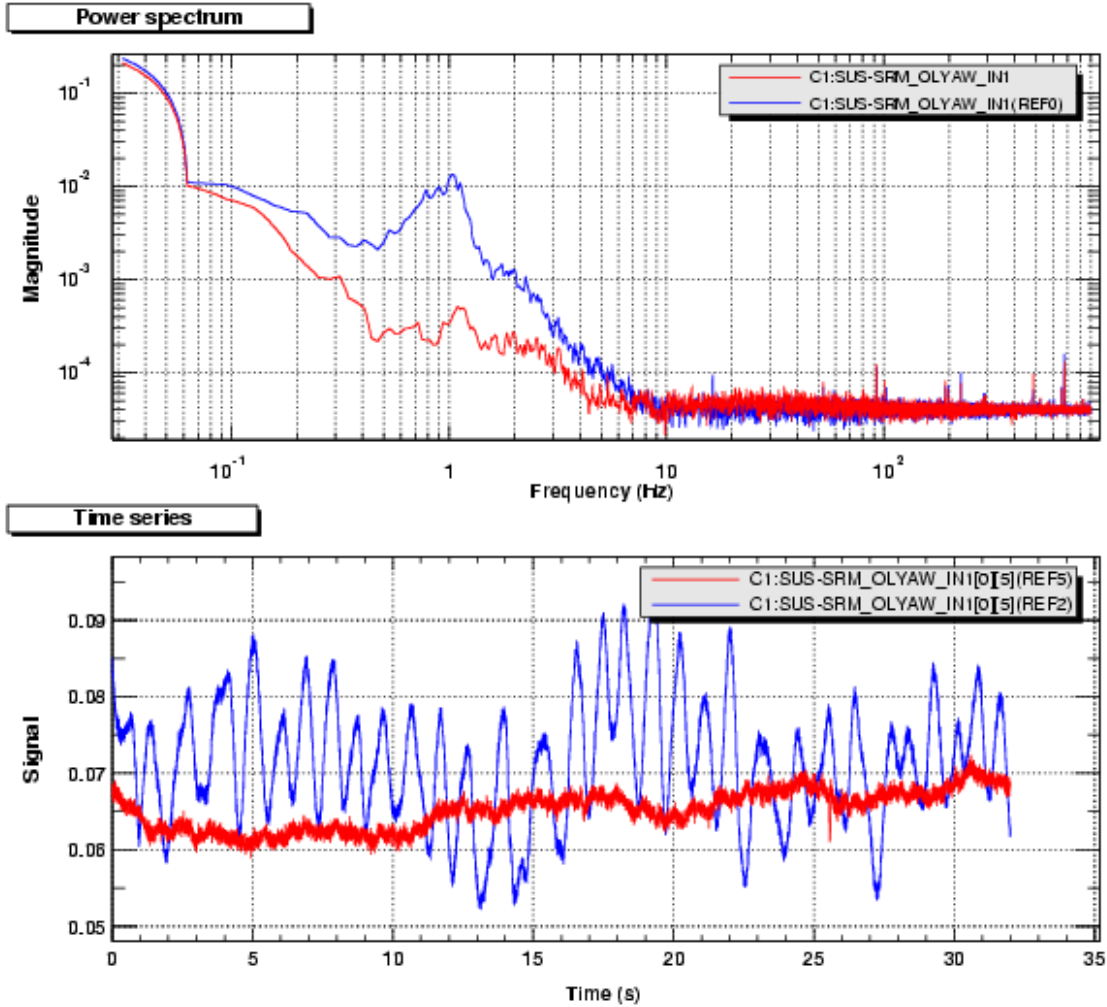


Fig. 36: In-loop noise spectra of SRM yaw

5 Future work

The Oplev control loop helps OSEM damp the optics properly in the region of pitch and yaw resonant frequencies. The Oplev servo appears to inject excess noise at higher frequencies which can hamper lock acquisition efforts; therefore, the filters have to be modified properly to suppress noises in that region of the frequency. The gains have to be adjusted so that the combination of the OSEM and Oplev control loops can perform at their best.

6 Conclusion

The Optical lever systems could be used with OSEM damping systems to control the motion of the suspended optics. It will help commissioning the 40 meter interferometer.

Appendix A

The correction of the wedge effect

Because the glass plate is slightly wedged, the wedge should be in vertical direction when calibrating horizontal (yaw) response of the QPD so that the initial beam and the exit beam are horizontally parallel.

To make sure the wedge is in vertical direction, the reflected beam from the glass plate was monitored as the part A in Fig. 37 was rotated. As it rotates, the reflected light also rotates and the trace was monitored on a material which refracts the beam (e.g. a piece of paper). When the reflected beam is at the top and the bottom of the circle, the wedge is in vertical direction. (See Figure 37)

The reason why the reflected beam was used is that it was more convenient to monitor the reflected beam because of the limited space on the Oplev table.

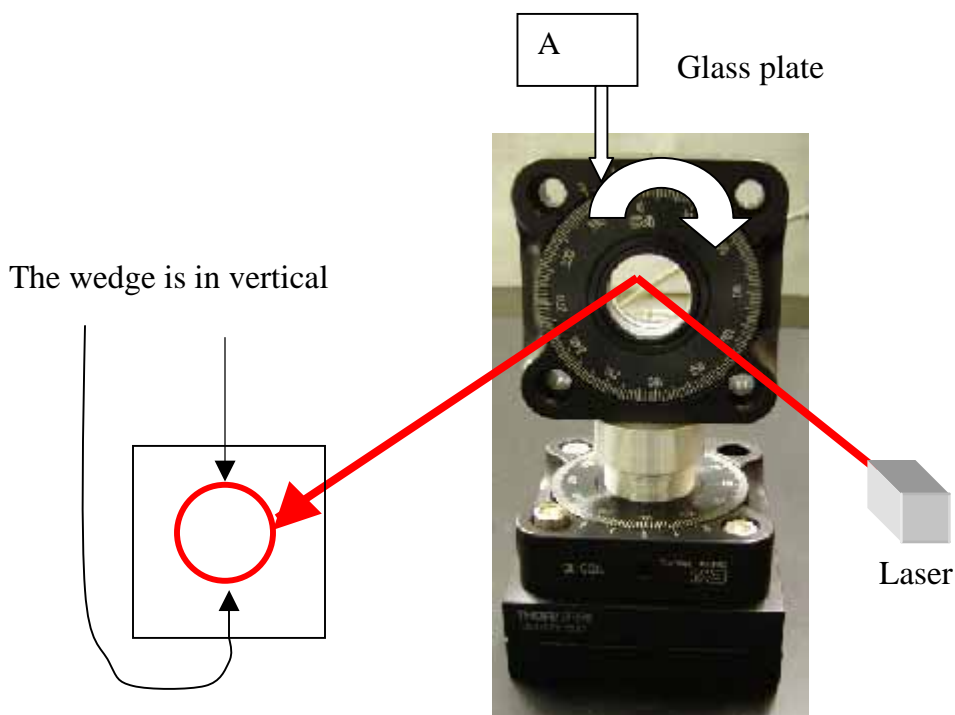


Fig. 37: Correction of the wedge effect